Diel dynamics of chlorophylls in high-nutrient, low-chlorophyll waters of the equatorial Pacific (180°): Interactions of growth, grazing, physiological responses, and mixing

Jacques Neveux,[1,2] Cécile Dupouy,[2,3] Jean Blanchot,[4] Aubert Le Bouteiller,[5] Michael R. Landry,[6] and Susan L. Brown[6]

Received 30 November 2000; revised 5 November 2002; accepted 2 April 2003; published 24 October 2003.

[1] In situ diel variations of extracted chlorophyllous pigments, beam attenuation by particles (c_p), and in vivo chlorophyll fluorescence (F_{iv}) were investigated during a 5-day time series in high-nutrient, low-chlorophyll waters of the equatorial Pacific (date line = 180°). Samples were taken hourly at 10 depths in the upper 100 m during the first 48 hours, then sampling frequency decreased to 3 hours. In the 30–70 m layer the integrated chlorophyll concentrations, c_p, and F_{iv} increased during the light period, but the minima and, especially, maxima were not fully synchronized. The lowest values of total chlorophyll *a* (Tchl *a* = chlorophyll *a* + divinyl-chlorophyll *a*) occurred around 5–6 hours, slightly (0–2 hours) before that of c_p and F_{iv}. Tchl *a* reached a maximum around 1500 hours ± 1 hour, clearly before c_p (1700 hours) and F_{iv} (1900 hours). In the 0–30 m layer, diel variations of the integrated chlorophyll concentrations, c_p, and F_{iv} were clearly out of phase. They showed a nocturnal increase in Tchl *a*, starting around midnight and peaking in early morning (0900 hours). In contrast, c_p increased only during the light period in the upper 30 m, and variations of F_{iv} were largely opposite to those of extracted Tchl *a*. Specific phytoplankton growth (μ_0) and grazing loss (g) rates were estimated from diel variations in the 30–70 m layer and compared to independent rate estimates from experimental incubations. These results are discussed in the context of physical processes and physiological responses of the cells to the daily photocycle. *INDEX TERMS:* 4231 Oceanography: General: Equatorial oceanography; 4227 Oceanography: General: Diurnal, seasonal, and annual cycles; 4271 Oceanography: General: Physical and chemical properties of seawater; 4855 Oceanography: Biological and Chemical: Plankton; 4815 Oceanography: Biological and Chemical: Ecosystems, structure and dynamics; *KEYWORDS:* equatorial Pacific, chlorophylls, HNLC waters, transimissometry, fluorescence, phytoplankton dynamics

Citation: Neveux, J., C. Dupouy, J. Blanchot, A. Le Bouteiller, M. R. Landry, and S. L. Brown, Diel dynamics of chlorophylls in high-nutrient, low-chlorophyll waters of the equatorial Pacific (180°): Interactions of growth, grazing, physiological responses, and mixing, *J. Geophys. Res.*, *108*(C12), 8140, doi:10.1029/2000JC000747, 2003.

1. Introduction

[2] Many phytoplankton, both prokaryotes and eukaryotes, display circadian rhythms related to the light-dark cycle (see *Suzuki and Johnson* [2001] for a minireview). Diel cycles are evident in photosynthetic capabilities, in vivo chlorophyll fluorescence, bioluminescence, nitrate reductase activity and phased cell division. These rhythms appear to be controlled by biological clocks which coordinate the different phases of cell growth and division and prepare cells in advance for predictable changes in environmental conditions.

[3] Spatial heterogeneity and water movements in the oceans are often unfavourable for observing in situ diel variations of phytoplankton. However, the diel signal is a well-recognized feature of the high-nutrient, low-chlorophyll region (HNLC) of the equatorial Pacific. In situ signals in chlorophyll fluorescence [*Setser et al.*, 1982; *Dandonneau and Neveux*, 1995; *Claustre et al.*, 1999], seawater light transmission [*Siegel et al.*, 1989; *Cullen et al.*, 1992; *Walsh et al.*, 1995; *Claustre et al.*, 1999] and picophytoplankton abundances and cellular properties [*Vaulot et al.*, 1995; *Durand and Olson*, 1996; *Blanchot et al.*, 1997; *Vaulot and Marie*, 1999; *André et al.*, 1999] are readily measured in this

[1]Observatoire Océanologique de Banyuls (CNRS-UPMC), Laboratoire Arago (UMR 7621), Banyuls sur Mer, France.
[2]Also at Institute de Recherche pour le Développement-Nouméa, Nouméa, New Caledonia.
[3]Laboratoire d'Océanographie Dynamique et de Climatologie (CNRS-IRD-UPMC), UMR 7617, UPMC, Paris, France.
[4]Institut de Recherche pour le Développement-Sainte Clotilde, Sainte Clotilde, La Réunion, France.
[5]Institute de Recherche pour le Développement-Nouméa, Nouméa, New Caledonia.
[6]Department of Oceanography, University of Hawaii at Manoa, Honolulu, Hawaii, USA.

0148-0227/03/2000JC000747$09.00

region, and they provide particularly important information for assessing the daily dynamics of phytoplankton stocks because they involve no containment artefacts. Nonetheless, interpretations of the diel signals must be done carefully as the observed variations reflect not only cyclical behaviors in biological processes, including growth and grazing, but potential changes in cellular physiology, community structure, food web interactions [*Fuhrman et al.*, 1985; *Landry et al.*, 1997; *Strom et al.*, 2000] and physical mixing of the euphotic zone.

[4] In the present study, diel variations of in vivo and extracted phytoplankton pigments, beam transmissometry by particles (c_p) and picophytoplankton were assessed over a 5-day period of fine-scale sampling at the equator, 180°. The resulting data describe the relationships of parameter variations relative to one another, as would be useful for constructing bio-optical models that reflect observed properties of natural systems [e.g., *Marra*, 1997]. In addition, diel changes in pigments, F_{iv} and beam c_p are used to derive growth and grazing rate estimates for the 30–70 m depth zone which are compared to independent estimates from experimental incubations. Clear changes of hydrological and chemical conditions occurred during the time series, related to the advection of the southward branch of a Tropical Instability Wave (TIW) through the sampling station [*Eldin and Rodier*, 2003]. This did not strongly modify biological community structure but could have affected diel trends in chl *a*, c_P and F_{iv} as well as growth and grazing estimates in the 30–70 m layer during the second 24-hour period of the time series.

2. Material and Methods

2.1. Sampling

[5] Phytoplankton pigment profiles and picoplankton optical properties were measured on the EBENE cruise (4–9 November 1996) during intensive time series sampling at the equator and dateline (0.08°S–0.04°N, 179.8°E–179.8°W). Seawater was collected with a CTD-rosette system composed of twenty-four 12 L Niskin bottles, a SeaBird SBE-911 Plus Conductivity-Temperature-Depth probe, an Aquatracka III in situ fluorometer (Chelsea Instruments), a SeaTech beam transmissometer (25-cm path length, λ = 660 nm), and a Biospherical Instruments QSP-200L Quantum Meter for measurement of Photosynthetically Available Radiation (PAR). During the first two days of the time series, samples were taken hourly at 10 depths (0, 10, 20, 30, 40, 50, 60, 70, 80 and 100 m). Subsequently, the sampling frequency was decreased to $\approx$ 3-hour intervals (8 casts d^{-1}), and 14–18 depths were sampled to 200-m depth.

2.2. Chlorophyll Pigment Analyses

[6] Seawater samples (500 mL) were filtered onto 47-mm Whatman GF/F fiber filters. For pigment extraction, the filters were dipped in a centrifuge tube containing 5.4 mL of 100% acetone (water retention in the filter bringing the final acetone concentration to ~90%) and ground with the fresh broken end of a glass rod. After a 12-hour extraction in the dark at 4°C, the tubes were centrifuged.

[7] Fluorescence properties of the extracts were measured on a Hitachi F4500 spectrofluorometer operating in the ratio mode. Slit widths were set to 5 and 10 nm for excitation and emission, respectively. Data acquisition was performed by recording the fluorescence emission spectra for each of 31 excitation wavelengths (3-nm increments from 390 to 480 nm). Emission spectra were recorded at 4-nm intervals from 615 to 715 nm, yielding 26 data points for each spectrum. Pigment concentrations were estimated from the resulting 806 data points (31 × 26) according to the least squares approximation technique [*Neveux and Lantoine*, 1993]. The spectrofluorometric method assumes that the sample extracts contain no more than 10 major pigments: chorophyll *a* (chl *a*), *b* (chl *b*) and *c* (chl *c*), divinyl chlorophyll *a* (dv-chl *a*) and *b* (dv-chl *b*) and phaeopigments derived from these five chlorophylls. Chl *c* is further assumed to be a mixture of chl c_1 and chl c_2.

2.3. Flow Cytometric Analyses

[8] Unpreserved seawater samples (120 mL) were analyzed for picophytoplankton on shipboard within 2 hours after collection with a FACScan flow cytometer (Becton-Dickinson) [*Blanchot and Rodier*, 1996; *Partensky et al.*, 1993]. For each picoplanktonic cell the forward and right angle light scatters as well as the fluorescence emitted by phycoerythrin (yellow-orange) and chlorophyll *a* or dv-chl *a* (red) were measured. Fluorescent microspheres (Polysciences) of 2.02-μm (FACScan) diameter were used as an internal reference. The list mode data were collected with Becton-Dickinson LYSYS-II software and analyzed with the free CYTOWIN software, an updated version of CYTOPC [*Vaulot*, 1989].

2.4. Phytoplankton Growth and Grazing Estimates from Beam *c* Transmissometry

[9] The beam attenuation coefficient "*c*" results from a linear combination of the effects of seawater (c_w), yellow matter (c_y) and particles (c_p). C_w is considered to be constant and equal to 0.364 m^{-1}, and c_y is assumed to be negligible in equatorial Pacific waters [*Walsh et al.*, 1995]. Therefore diel variations of *c* result primarily from changes in the nature and concentration of particles (i.e., $c_p = c - 0.364$). Since the relationship $c_p$versus particulate organic carbon (POC) appears linear in the Pacific Ocean [*Claustre et al.*, 1999; *Bishop*, 1999], diel c_p variations are examined in terms of diel POC variations. Nevertheless, the choice of a conversion factor is problematic, with *Claustre et al.* [1999] reporting a c_p to POC conversion factor 2.4 times higher than that of *Bishop* [1999]. This discrepancy was due to different modes of sampling: bottles [*Claustre et al.*, 1999] versus a large-volume in situ filtration system [*Bishop*, 1999]. An even higher discrepancy (mean = 3.2) was noted for the two POC sampling approaches during EqPac, but its origin was then considered unresolved [*Dunne et al.*, 1997]. During EBENE, independent estimates of autotrophic particular carbon (APC) from cell counts, cellular biovolumes and community structure [*Brown et al.*, 2003] provide an additional perspective on carbon conversions. Near the equator (1°N–1°S), APC/Tchl *a* ratios varied from 84 to 149 (mean = 113) in the upper 40 m and ranged from 31 to 81 (mean = 64) between 50 and 80 m [*Brown et al.*, 2003]. On the basis of *Bishop*'s [1999] relationship between c_p and POC, the calculated POC/Tchl *a* ratios would have been lower than those for APC/Tchl *a* at similar depths. In addition, they would not

have accounted for the significant carbon contributions of small heterotrophs (bacteria, ciliates, flagellates) and detritus — about one third of living biomass in the microbial size fraction [*Brown et al.*, 2003; *Claustre et al.*, 1999] and 40% of total POC [*Claustre et al.*, 1999], respectively. Because *Claustre et al.*'s [1999] conversion factor [POC (mg m^{-3}) = c_p^*500] gave results more compatible with the microscopical analyses of living biomass (section 3.4 below), we used it to transform c_p to POC equivalents.

[10] We estimated phytoplankton growth and grazing rates from c_p variations at 60 m for the first 48-hour sampling period when very clear diel variations were observed and hourly frequency sampling was performed. For these, the period was divided into four parts: 1) a decreasing portion (D_1) from 1700 hours (4 November) to 0700 hours (5 November); 2) an increasing portion (I_1) from 0700 to 1600 hours (5 November), 3) a decreasing segment (D_2) from 1600 hours (5 November) to 0600 hours (6 November); and 4) an increasing part (I_2) from 0600 to 1700 hours (6 November). The advection of the TIW front occurred 2–3 hours after the beginning of the D_2 phase. These same four parts were also determined for integrated c_p in the 0–30 m (>10% of surface PAR) and 30–70 m (1–10% of surface PAR) depth ranges, with only slight differences due to depth-related phase shifts in the timing of the c_p minima and maxima. For each part, exponential ($y = a e^{bt}$) regressions were calculated from the data points, with y and t representing c_p and time, respectively (a and b are constants). Following a simple growth/grazing model [*Siegel et al.*, 1989], we assumed that c_p changes during the D_1 and D_2 (dark) periods were due only to grazing. Our estimated rates of change (b) are therefore per hour estimates of grazing-associated losses (g, h^{-1}). Similarly, the exponential rates of change (b) for the I_1 and I_2 regressions represent hourly estimates of the rate difference between growth and grazing ($\mu_o - g$; h^{-1}). Specific growth rates were subsequently computed from the differences in daily D and I regressions, assuming that grazing rates were similar in the light and dark. Hourly rates were expressed on a daily basis following the assumptions that grazing occurred over 24 hours while growth was restricted to the light (I) periods.

2.5. Phytoplankton Growth and Grazing Rate Estimates From Diel Variations of in Situ Pigments and in Vivo Fluorescence

[11] As discussed further below, the in situ observations of pigment variations in the study region also lend themselves to interpretation of the daily cycle of growth and grazing, assuming balanced growth and some synchronicity in the patterns of cell division. To assess the possibility that phytoplankton growth and grazing rates could be estimated from these variations, the 48-hour hourly sampling period at 60 m was divided into four parts similar to those for c_p above but differing slightly in timing: 1) D_1 = 1400 hours (4 November) to 0500 hours (5 November); I_1 = 0500 to 1400 hours (5 November); D_2 = 1400 hours (5 November) to 0600 hours (6 November); and I_2 = 0600 to 1400 hours (6 November). As above, similar periods of increasing and decreasing integrated concentrations were also defined for the 30–70 m depth range. For each period and for each chlorophyll pigment, exponential regressions were performed to compute mean hourly estimates of μ_o and g.

[12] Similar analyses were performed using in vivo fluorescence (F_{iv}) data for the 30–70 m depth range with the following timing for the different phases: 1) D_1 = 1900 hours (4 November) to 0700 hours (5 November); I_1 = 0700 to 1900 hours (5 November); D_2 = 1900 hours (5 November) to 0700 hours (6 November); and I_2 = 0700 to 1900 hours (6 November).

2.6. Diel Grazing Experiments

[13] To complement in situ observations of the daily fluctuations in population abundances and pigments in the EBENE study, an attempt was made to assess the diel pattern in grazing on *Prochlorococcus* cells from shipboard incubation studies during the first day-night period (i.e., corresponding approximately to D_1 and I_1 above). These experiments were conducted with water collected from each of two depths, 30 and 60 m. For each sampling depth, the full day cycle was divided into four parts, with incubation times from 1630–2230, 2200–0420, 0400–1010, and 1100–1700 local time. Eight experiments were conducted in total. Over the course of the experiments, the ambient environment was sampled at 3-hour intervals at 30- and 60-m depths to elucidate the diel abundance cycle of protistan grazers, dominated by nonpigmented nanoflagellates [*Brown et al.*, 2003].

[14] Seawater was collected from depth immediately prior to the start of each experiment from the same CTD samples used to define the in situ pigment signal. Part of the sample was filtered as gently as possible through a 45-mm, acid-washed polycarbonate filter 1-μm pore size into a clean polycarbonate flask using a hand held vacuum pump (~5 cm Hg vacuum pressure). This was assumed to be predator free [e.g., *Calbet and Landry*, 1999]. The remaining sample was used without filtration, and therefore contained *Prochlorococcus* and protistan grazers in natural abundances. To simultaneously assess the grazing pressure on a nongrowing tracer, fluorescently labeled bacteria (FLB = Vibrio damsella ~ 1.1 μm in size, prepared according to *Sherr et al.* [1987]) were added equally (~10,000 cells mL^{-1}) and gently mixed into the prefiltered and unfiltered seawater samples. The water for each treatment condition was then divided into six 60-mL polycarbonate centrifuge tubes, with 2 tubes sacrificed for initial samples and 4 replicates incubated in shipboard incubators (light blue Plexiglas tint 2069 for 30 m; dark blue tint 2424 for 60 m) [*Laws et al.*, 1990] screened with neutral density fabric to ambient light levels.

[15] Initial and final samples from the experiments were preserved with paraformaldehyde (0.5%) and frozen in liquid nitrogen for later analysis. Population abundances of FLB and *Prochlorococcus* cells were enumerated in 100-μL subsamples with a Coulter EPICS 753 flow cytometer equipped with dual 5W argon lasers, MSDS II automatic sampling, a Biosense flow cell and CICERO Cytomation software [*Landry et al.*, 1995]. List mode files were analyzed using CYTOPC software [*Vaulot*, 1989]. Heterotrophic protists were enumerated from 50-mL samples preserved with 0.5% paraformaldehyde, stained with 25 μl of 0.033% (w/v) proflavin and 10 μg mL^{-1} DAPI, and concentrated on 0.6-μm black polycarbonate filters. The filters were mounted on glass slides and analyzed with a Zeiss epifluorescence microscope and image analysis system software [*Brown et al.*, 2003].

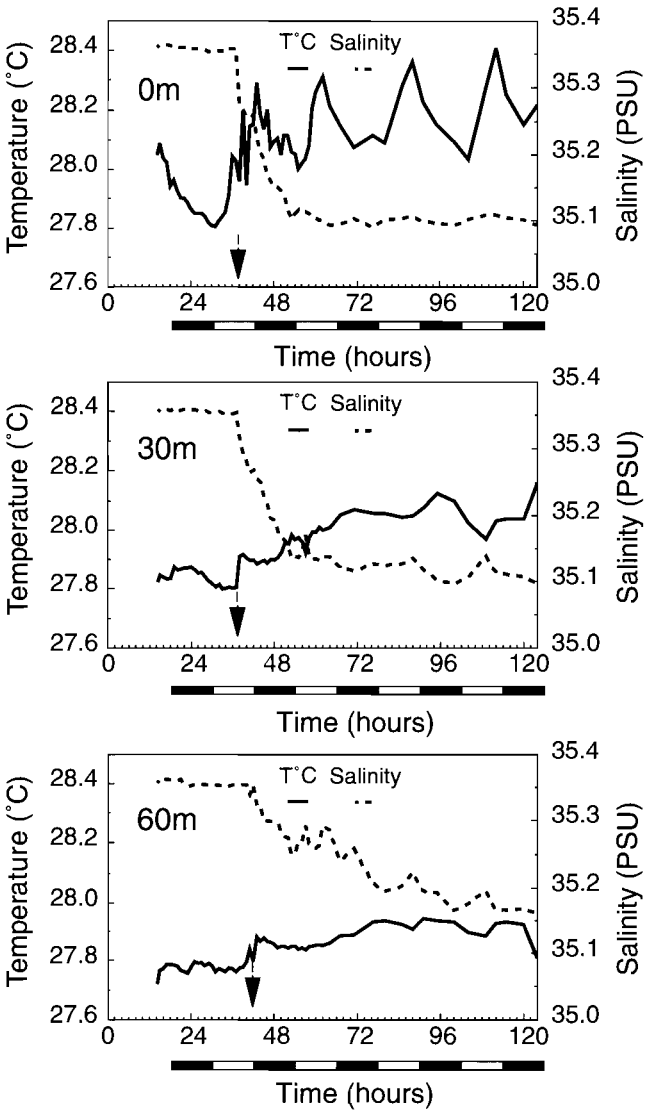

Figure 1. Temperature and salinity at 0, 30, and 60 m depths during the 5-day time series at the equator (180°). Arrows indicate the passage of the Tropical Instability Wave.

[16] The natural log of the ratios of final to initial mean population estimates were used to compute exponential rates of change for each treatment, depth and incubation period. Mean grazing estimates were determined as the difference between hourly rates of change for the prefiltered treatments (μ_o) and the corresponding natural water treatments ($\mu_o - g$) (i.e., $g = (\mu_o) - (\mu_o - g)$). For FLB, the prefiltered treatments gave μ_o estimates varying only slightly around zero, indicating insignificant grazing losses and no effect of sunlight bleaching on the subsequent analysis of the stained cells. For *Prochlorococcus*, the observed rates of change in the prefiltered treatments are presented as growth (μ_o) rate estimates.

3. Results

3.1. Hydrological Variability

[17] All sampling times are relative to 14h15 local time on 4 November ($=t_o$). Surface water temperatures and salinity averaged 28.06°C and 35.22 psu respectively (temperature range: 27.80°–28.41°C; salinity range: 35.09–35.36 psu). Salinity was quasi-constant during the first 24 hours (mean: 35.35 psu; coefficient of variation: 0.05%) then it decreased gradually between 24 and 36 hours and remained constant (mean: 35.10 psu; coefficient of variation: 0.02%) until the end of the time series (Figure 1). This salinity front was accompanied by a sharp decrease in nitrate from 3.5 to 1.7 μM [*Eldin and Rodier*, 2003] and by a 0.25°–0.3°C increase in temperature relative to the previously observed diel cycle of daytime warming and nocturnal mixing (cooling). These physical changes, extending to 80-m depth, were linked to the advection of the southward branch of a Tropical Instability Wave (TIW) [*Eldin and Rodier*, 2003]. Below 30 m, however, the sharp salinity decrease was delayed from 1 to 4 hours, with its amplitude evolving more slowly and weaker at increasing depths (Figure 1). At 60 m, nitrate concentrations varied from a mean of 3.6 μM (coefficient of variation = 6.4%) in the first 28-hour period to a mean of 2.8 μM (coefficient of variation = 4.8%) after 30 hours.

[18] To assess temporal variability in water column stability, the coefficients of variation (CV_d) of density (σ_θ values averaged over 2-m depth intervals) were determined in different layers. CV_d showed diel variations with maximum stratification in the daylight period around 1500 hours ± 1 hour because of the diurnal warming of

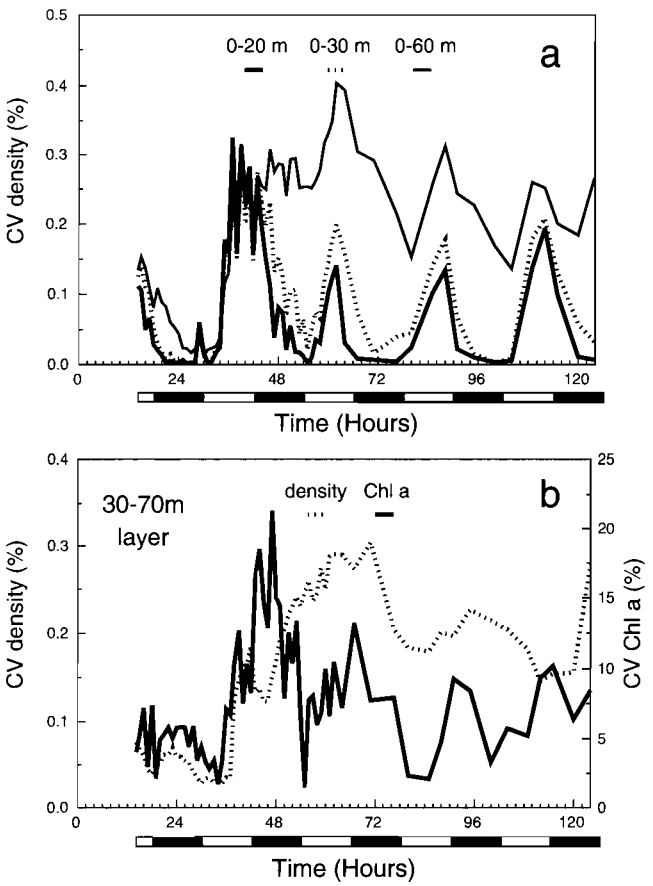

Figure 2. Coefficient of variation (CV_d) of the density (σ_θ) in different layers during the 5-day time series at the equator (180°): (a) 0–20 m, 0–30 m, and 0–60 m; and (b) in the 30–70 m layer including a comparison with the coefficient of variation of the chlorophyll *a* (chl *a*) concentration.

near-surface water (Figure 2a). Vertical mixing was more intense at the end of the first sampling night ($CV_d < 0.05\%$ at sunrise in the 0–80 m layer). During the following nights only the upper 20–30 m was uniformly mixed. This difference is evident in the CV_d of the 30–70 m layer (Figure 2b), which was low during the first 24 hours (~0.05%), increasing significantly (0.1–0.3%) thereafter. The CV for chl *a* concentration followed CV_d for the first part of the time series, but was out of phase in subsequent sampling.

3.2. Diel Variations of Chlorophyll Concentrations

[19] The time series observations were divided into two parts according to sampling frequency. At the beginning (1415 hours on 4 November) of the initial 48-hour hourly sampling the vertical profile of chlorophyll showed a maximum at 50–60 m. In the following hours, Tchl *a* concentration decreased, particularly below 30 m, and the profile became homogeneous in the 0–80 m layer during the night (Figure 3a). At sunrise on 5 November, Tchl *a* (chl *a* + dv-chl *a*) increased at all depths to a maximum at 0800–1100 hours in the surface layer (0–30 m). The maximum appeared later (1300–1500 hours) at 40–70 m. This pattern was also illustrated in the diel variations of Tchl *a* at 0 and 60 m (Figure 6a). As previously noted, nocturnal mixing after the first 24-hour sampling occurred only in the 0–30 m layer. A Tchl *a* minimum was observed at the end of the night between 40 and 70–80 m, appearing sooner above 40 m (around midnight). Similar cycles occurred during the next daylight period although the maximum biomass level was lower, particularly in the upper 30 m. During the last three days, the 3-hour sampling frequency showed pigment variations similar to those observed during hourly sampling, but the actual times and absolute values of the maxima and minima could not be determined as clearly. Similar variations were observed for chl *a* and dv-chl *a* (Figures 3b and 3c) alone and for accessory chlorophylls (chl *b* and *c*; Figures 4a and 4b). However, in the 0–30 m layer, the nocturnal minimum of dv-chl *a* concentration tended to occur sooner than that of chl *a*. Dv-chl *b* concentration was never significant in the upper 60 m and was largely restricted to depths below 80 m. However, a few erratic occurrences of low but significant dv-chl *b* concentrations were noted at 70 m.

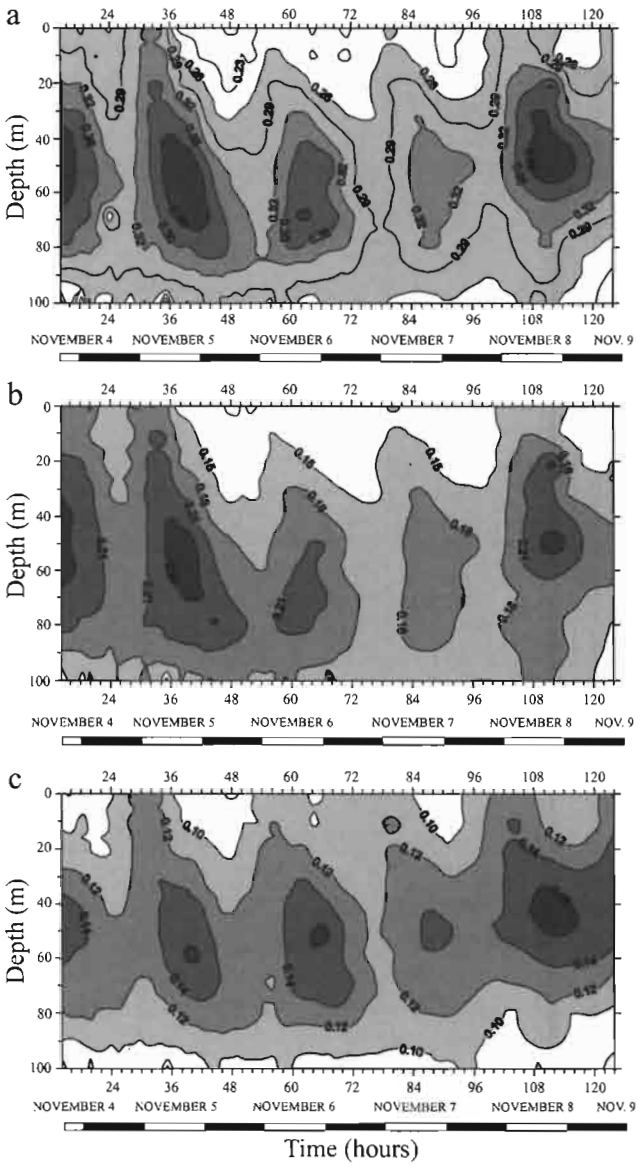

Figure 3. Diel variations of (a) total chlorophyll *a* concentration (Tchl *a*) and its two components, (b) chlorophyll *a* (chl *a*), and (c) divinyl chlorophyll *a* (dv-chl *a*) during the 5-day time series at the equator (180°); EBENE cruise (4–9 November 1996).

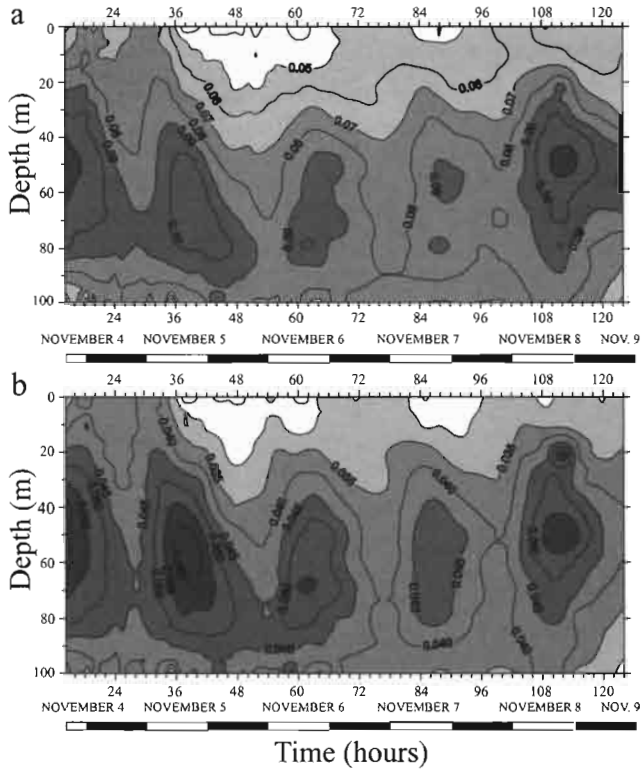

Figure 4. Diel variations of accessory chlorophylls: (a) chlorophyll *c* (chl *c*) and (b) chlorophyll *b* (chl *b*) during the 5-day time series at the equator (180°).

3.3. Pigment Ratios

[20] Fluctuations in the pigment ratios of the bulk phytoplankton community reflect changes in both the community

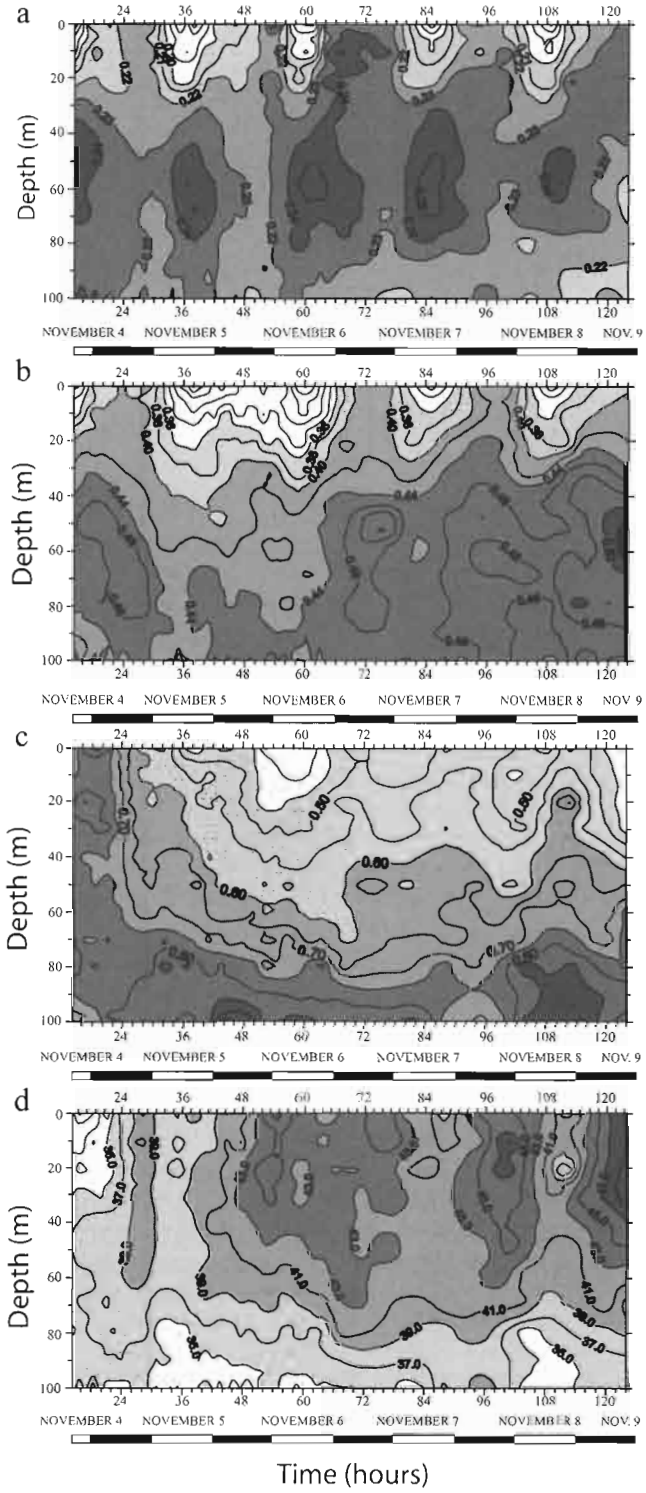

Figure 5. Diel variations of pigment ratios during the 5-day time series at the equator (180°): (a) chl *c*/chl *a*, (b) chl *b*/chl *a*, (c) chl *b*/dv-chl *a*, and (d) percentage of dv-chl *a* calculated as dv-chl *a** 100/(chl *a* + dv-chl *a*).

structure and the relative pigment concentrations inside the different types of cells (Figure 5). These fluctuations are not easily interpreted since cellular pigment ratios are usually unknown. Nevertheless, diel variations were particularly clear for the chl *c*/chl *a* ratio (Figures 5a and 6b). Between 0 and 30 m, minimum values were observed at noon and maximum values at night. The reverse was true at greater depths, down to 80 m. Similar observations were noted in the upper layer for the chl *b*/chl *a* ratio (Figure 5b), but diel variations were not clear at depth. This could mean that chl *b* was not present in chlorophytes, but in *Prochlorococcus marinus* which contain dv-chl *a* [*Bidigare and Ondrusek*, 1996; section 4.1]. However, the diel pattern was still unclear for the chl *b*/dv-chl *a* ratio (Figure 5c). On a daily basis, the mean integrated pigment ratio exhibited minor variations in the 30–70 m layer (5–6% for chl *b*/chl *a* and less than 1% for the chl *c*/chl *a* ratio), but the chl *c*/chl *a* ratio increased significantly in the 0–30 m layer, from 0.208 to 0.226, with the arrival of the hydrological front.

[21] Overall, the percentage of dv-chl *a*, defined as dv-chl *a**100/Tchl *a*, showed a slight increase during the time series. However, a diel variation was superimposed on this trend in the upper layer (0–60 m), particularly visible during the last two days of the time series (Figure 5d). The dv-chl *a* percentages were minimum during the day, increasing at dusk and through the night. This variation might be related to differences in the relative grazing pressure on *Prochlorococcus* and eukaryotes, the maximum dv-chl *a* percentage reflecting a more active nighttime

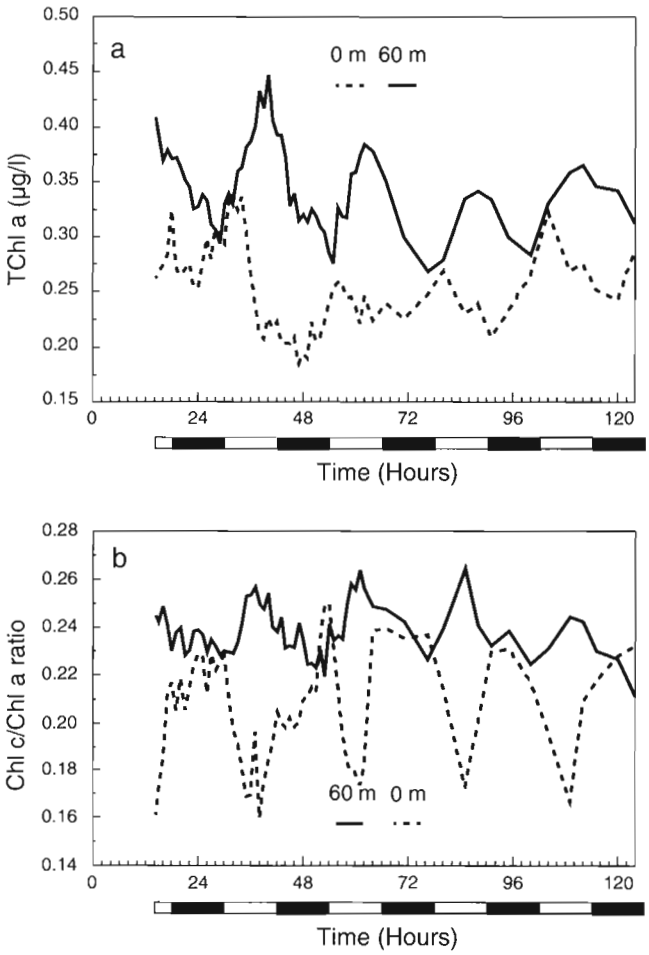

Figure 6. Diel variations at 0 and 60 m during the 5-day time series at the equator (180°): (a) concentration of total chlorophyll *a* (Tchl *a*) and (b) chl *c*/chl *a* ratio.

grazing pressure on cells containing chl *a*. For example, the larger, vertically migrating zooplankton would be expected to feed more efficiently on larger eukaryotic phytoplankton. During time series sampling at the EBENE equatorial station, mesozooplankton biomass showed a 1.5-fold nocturnal increase in the 0–100 m layer (2100 to 0300-hours mean ± standard deviation = 18.4 ± 3.4 mg dry wt m^{-3}) relative to daytime levels (0900–1500 hours; 11.9 ± 2.1 mg dry wt m^{-3}) [*Champalbert et al.*, 2003]. Similar diel variations in mesozooplankton biomass have been reported in equatorial waters at 140°W [*Roman et al.*, 1995] and 150°W [*Le Borgne and Rodier*, 1997].

3.4. Diel Variations of c_p and in Vivo Chlorophyll Fluorescence

[22] Diel variations of transmissometry c_p and F_{iv} were also distinct in the time series, but they did not match exactly the pattern for extracted pigments. For example, the broad maxima and minima of integrated F_{iv} were strongly out of phase with integrated Tchl *a* in the upper 30 m (Figure 7a). Moreover, the depressed peak heights observed for the extracted pigments during the third and fourth daylight periods were reflected in the contemporaneous minima of F_{iv} but not in the F_{iv} maxima. Therefore the amplitudes of the diel variations increased for F_{iv} and contracted for Tchl *a* during this period. For the 30–70 m (Figure 7b) depth integrations, in contrast, the amplitudes of diel variations in the two parameters matched more closely with the F_{iv} maxima, following extracted Tchl *a* by only a few hours.

[23] In Figure 8, the diel signal in integrated c_p is converted to Particulate Organic Carbon (POC) equivalents using the linear relationship of *Claustre et al.* [1999] and examined relative to integrated Tchl *a*. For the upper 30 m, POC estimates from c_p lagged Tchl *a* by ~8 hours, with POC increasing from early morning through the daylight period compared to the nocturnal increases in Tchl *a* (Figure 8a). Despite the temporal offset, however, the relative amplitudes of the diel variations, including the day-to-day differences in peak heights were closely matched. This was also evident in the somewhat more synchronous variations of integrated POC and Tchl *a* in the 30–70 m depth interval, except during day 4, where the observed amplitude for Tchl *a* was large relative to that of POC (Figure 8c). For both depth ranges, the differences in timing of the integrated POC and Tchl *a* maxima and minima led to approximately a 50% variation in the POC:Tchl *a* ratio (Figures 8b and 8d). For the 0–30 m depth integrations, the ratio varied from about 120 in the early morning to 180 at the end of the daylight period. At 30–70 m, the range was from 90 to 130, and the maxima and minima were broader in time with sharp transitions in the later part of the night and in the afternoon. Conversion of c_p to total POC using the Claustre et al.'s factor led to POC values about 30% higher than carbon estimates for autotrophic cells in the upper depth strata, and 70% higher at depth [*Brown et al.*, 2003]. Nonetheless, the POC estimates from c_p are less than what they would need to be to account for microscopical estimates of autotropic and heterotropic cells as well as a substantial amount of detritus (42% of total POC during OLIPAC) [*Claustre et al.*, 1999]. These discrepancies might be due to uncertainties inherent to the different

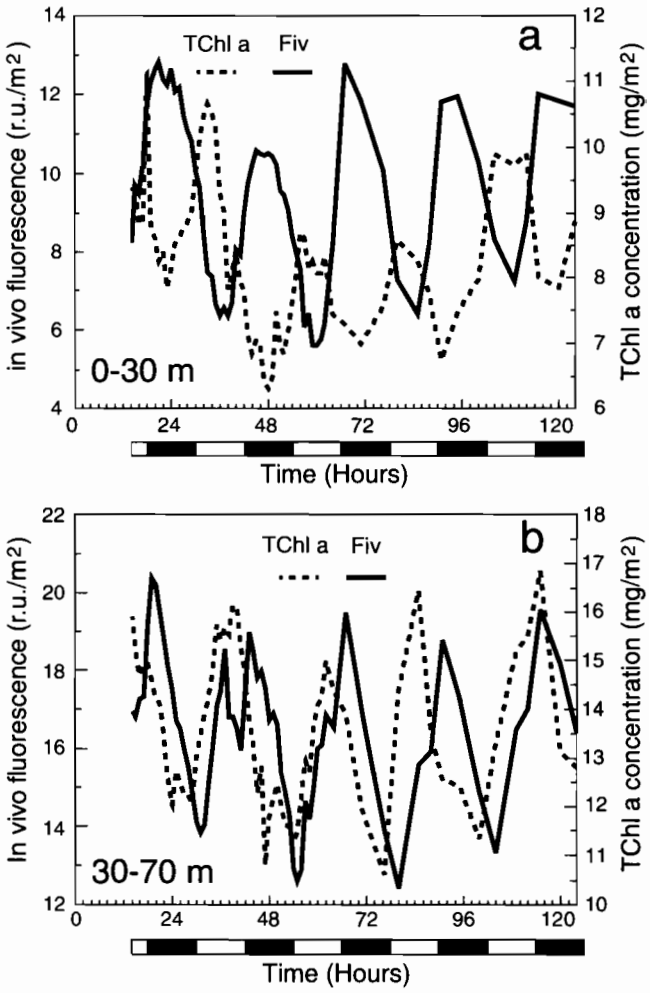

Figure 7. Diel variations of integrated in vivo chlorophyll fluorescence in the (a) 0–30 m and (b) 30–70 m layers during the 5-day time series at the equator. Comparison with diel variations of integrated total chlorophyll *a* (dashed line).

methodologies, such as inaccuracies in cell C:biovolume conversions, POC losses of small particles (bacteria, detrital carbon) on GF/F filters, or the acid treatment to which *Claustre* subjected the filters (personal communication). However, *Brown et al.* [2003] used conservative conversion factors, among the lowest in the literature. Moreover, direct estimates of total particulate carbon taken at the equator on EBENE samples [*Takayama and Suzuki*, personal communication] gave a slope with c_p only a little bit higher (564) than *Claustre*'s estimate.

3.5. Growth and Grazing Estimates From Diel Variations in Pigments, in Vivo Fluorescence, and C_p

[24] Our analyses of phytoplankton growth and grazing focus on the diel variations at 60 m (Figure 9a), approximately the depth of the chlorophyll maximum, and in the integrated zone from 30 to 70 m (Figure 9b). Pigment changes were roughly similar at the different sampling depths in this zone, although the maxima tended to occur a little later with increasing depth.

[25] In the equatorial Pacific, the main phytoplankton populations are picoplankton (cell sizes < 2 μm) [*Le Bouteiller et al.*, 1992; *Le Borgne et al.*, 1999], which

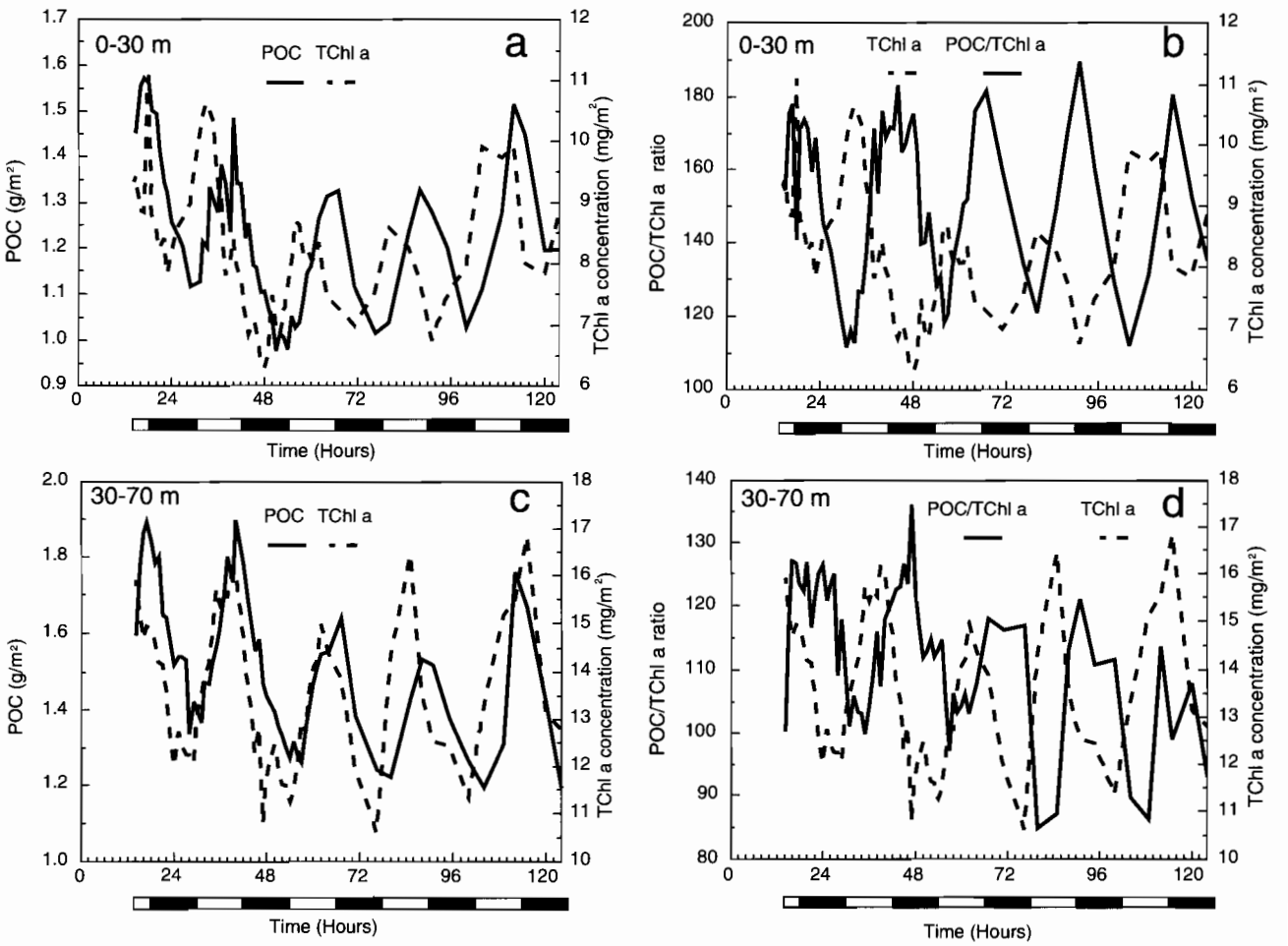

Figure 8. Diel variations of integrated (a) and (c) particulate organic carbon (POC) and (b) and (d) POC/Tchl *a* in the 0–30 m and 30–70 m layers during the 5-day time series at the equator. Comparison with diel variations of integrated total chlorophyll *a* (dashed line).

divide more or less synchronously [*Vaulot et al.*, 1995; *Blanchot et al.*, 1997]. In previous studies as well as on the present cruise (J. Blanchot et al., unpublished manuscript), cell division and maximum abundances occurred late in the afternoon or during the night, with different periods of division for *Prochlorococcus*, *Synechococcus* and picoeukaryotes. At 60-m depth, hourly variations of in situ chlorophyll concentrations showed two main phases in the diel cycle: a rapid increase from sunrise (~0500–0600 hours) to 1400–1500 hours, then a regular decrease until the following sunrise. Since the cells are largely synchronized with respect to the light-dark cycle, we examined the implications of the observed diel variations in pigment concentrations on rate estimates of phytoplankton growth and grazing losses for the light (I) and dark (D) phases of the cycle, as described in section 2.5.

[26] Data regressions typically showed high determination coefficients (r^2; Table 1). At 60 m, the best fits were obtained for the chl *c* concentration, with r^2 always higher than 0.80, and the worst for dv-chl *a* during the D_1 and D_2 phases (r^2 = 0.62 and 0.69). Chl *c* variations gave the highest estimates of g (0.65–0.88 d^{-1}) and μ_0 (0.62–0.71 d^{-1}) (Table 1). In the 30–70 m layer, g and μ_0, deduced from the variations of all integrated chlorophylls, were close but generally slightly lower than those calculated at 60 m, with values around 0.5–0.7 d^{-1}. Low grazing rate estimates (0.23–0.30 d^{-1}) were observed for dv-chl *a* during D_1.

[27] Although the timing of the D and I phases of the diel variations in integrated c_p differed from those of the pigments, the μ_0 and g rate estimates were roughly comparable (0.5–0.7 d^{-1}; Table 2). In the 30–70 m layer, similar observations could be made from diel integrated F_{iv} variations (0.6–0.8 d^{-1}) with high r^2 coefficients (>0.92), except for the I_1 phase (0.5; Table 3). However, this phase exhibited a double peak structure which was not observed in integrated Tchl *a* and c_p variations. The initial increase from 0700 to 1300 hours was particularly well represented by the exponential growth assumption (r^2 = 0.98). Extrapolating this increase to a 12-hour growth period would lead to a μ_0 of 1.01 d^{-1}, i.e., higher than observed for integrated c_p and extracted pigments. For the 0–30 m layer, integrated c_p variations indicated similar g values to those in the 30–70 m depth range (particularly for the D_2 phase), but μ_0 values were slightly lower (0.4–0.5 d^{-1}).

3.6. Effect of the Tropical Instability Wave on Community Structure, Growth, and Grazing Rates

[28] To interpret diel in situ variations in terms of quantitative biological processes, the natural community needs to be sampled under relatively constant physico-chemical

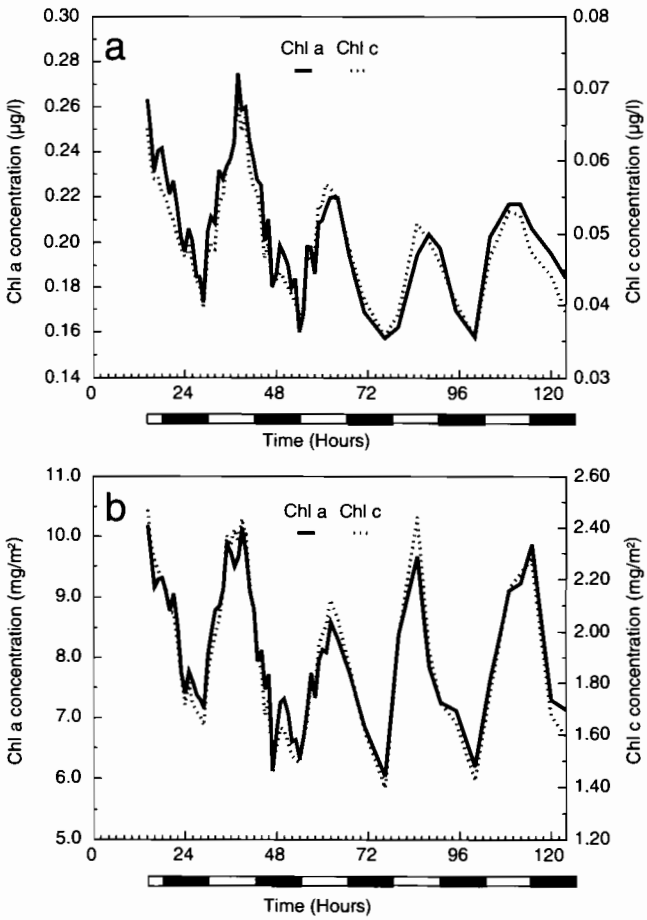

Figure 9. Diel variations of chlorophyll *a* (chl *a*) and chlorophyll *c* (chl *c*) during the five days time series at the equator: (a) concentrations at 60 m and (b) integrated concentration from 30 to 70 m.

conditions. These criteria seem clearly achieved during the first 24 hours (28 hours at 60-m depth) and after 36 hours, but the passage of a TIW front between 24 and 36 hours modified slightly the hydrological and chemical conditions during the present time series. This transition was not accompanied by drastic changes in phytoplankton community structure and biomass in the 30–70 m layer. In this layer, comparative estimates of mean daily pigment concentrations before and after the passage of the hydrological front showed only a slight decrease of integrated chl *a* (−10%), chl *b* (−4%), chl *c* (−9%). Since the integrated dv-chl *a* exhibited a slight increase (+9%), mean Tchl *a* was not strongly affected (−2%) and the mean percentage of dv-chl *a* increased from 38 to 42.5%. Cell counts by flow cytometry confirmed a slight decrease of eukaryotes and a slight increase of *Prochlorococcus* spp. (data not shown). Moreover, the accessory pigment to chl *a* ratios were relatively stable, suggesting that eukaryotic populations were not strongly modified. The passage of the front occurred during the D_2 phase could have led to an overestimation of g and consequently of μo from chl *a* (or accessory chlorophylls) during the I_2 phase and conversely from dv-chl *a*.

[29] In the 0–30 m layer, the decreases of mean integrated chl *a* (28%), chl *b* (23%), chl *c* (18%) and Tchl *a* (13%) exceeded those in the 30–70 m layer, whereas the increase of integrated dv-chl *a* was slightly lower (6%). The increase of the percentage of the integrated dv-chl *a*, from 36 to 44%, was slightly higher than in the 30–70 m layer.

[30] Mesozooplankton biomass was not sampled during the passage of the TIW front through our study site. Most vertical net hauls were made after the wave passed, but the difference between the one sample taken before and the others suggested a biomass increase of about 50% [*Le Borgne et al.*, 2003]. This contrasts with the fivefold increase reported during EqPac in October 1992 [*Roman et al.*, 1995]. However, in the latter case, the physico-chemical and biological variations during the passage of the TIW were opposite to those observed during the present study and corresponded to the advection of a northern TIW branch. Considering the relatively weak mesozooplankton grazing impact estimated on Tchl *a* (3–4%) and on >3-µm chl *a* (maximum = 15.7% d^{-1}) during EBENE by the gut fluorescence method [*Champalbert et al.*, 2003], their biomass variation likely had a minor influence on Tchl *a*.

[31] For heterotrophic protists, the interpretation of the TIW front passage on grazer abundance is confounded by the presence of one high nightime (0130, 30-m) value in the diel sampling conducted prior to the wave's arrival (Figure 10). The elevated abundance at this sample point is attributable to an unusual concentration of 5–7 µm thecate dinoflagellates compared to samples taken 3 hours before and 3 hours after, and it is also the only time at which abundances for samples collected at 30 and 60 m were markedly different. If one assumes that this point is spurious (i.e., it should be more like 60-m abundance at the same time), then the three samples collected after the TIW passage on 7–9 November appear to exceed by about 50% those collected during the same time of day before the TIW. If one does not discount this point, there is essentially no difference in the early morning, mean abundance of micrograzers before and after the TIW.

3.7. Experimental Determinations of Grazing Rates

[32] Overall, results from the size fractionation experiments (Table 4) were not sufficiently consistent to reveal a diel grazing pattern. On the basis of the rate estimates for *Prochlorococcus* at 30 m, for example, grazing activity appeared to be more concentrated during the nighttime. However, this was not evident at 60-m depth, where the calculated rates for the 2200–0420 incubation were lowest while the other estimates were uniformly high. Likewise, while the grazing activities on FLB followed that of *Prochlorococcus* at 60 m, the two rate measurements did not covary at 30 m. Mortality rate estimates were also not significantly related to protistan grazer abundances measured at the start of each incubation. However, grazer densities were relatively constant for all experiments (mean = 735 ± 118 cells mL^{-1}), with the set-up times missing the peak protist abundance in samples collected at 0130 (Figure 10). Due largely to the influence of the 0130 time points, diel sampling gives the visual impression of a midday to midnight increase in protistan grazers. Nonetheless, the 30% difference between mean nightime (1800–0600 hours; 840 ± 440 cells mL^{-1}) and daytime (640 ± 170 cells mL^{-1}) abundances from the combined 30- and 60-m samples is not statistically significant ($p = 0.20$; Mann-Whitney U test).

Table 1. Exponential Regressions $y = ae^{bt}$ of Pigment Concentrations (y) as a Function of Time (t) at the Equator (180°)[a]

Pigment	r^2	a	b	b_0	g
		D_1, 60 m (n = 16)			
chl *a*	0.93	0.259	−0.0240		−0.58
chl *b*	0.84	0.115	−0.0200		−0.48
chl *c*	0.97	0.063	−0.0279		−0.65
dv-chl *a*	0.62	0.143	−0.0099		−0.23
Tchl *a*	0.93	0.401	−0.0188		−0.45
		D_1, 30–70 m (n = 16)			
chl *a*	0.93	10.05	−0.0235		−0.56
chl *b*	0.89	4.55	−0.0242		−0.58
chl *c*	0.97	2.44	−0.0283		−0.68
dv-chl *a*	0.75	5.70	−0.0124		−0.30
Tchl *a*	0.92	15.74	−0.0193		−0.42
		D_2, 60 m (n = 17)			
chl *a*	0.91	0.267	−0.0298		−0.71
chl *b*	0.88	0.115	−0.0315		−0.75
chl *c*	0.94	0.067	−0.0371		−0.88
dv-chl *a*	0.69	0.171	−0.0234		−0.57
Tchl *a*	0.90	0.438	−0.0272		−0.65
		D_2, 30–70 m (n = 16)			
chl *a*	0.82	9.62	−0.0302		−0.72
chl *b*	0.80	3.94	−0.0278		−0.67
chl *c*	0.85	2.31	−0.0352		−0.84
dv-chl *a*	0.65	6.10	−0.0181		−0.43
Tchl *a*	0.80	15.69	−0.0252		−0.60
Pigment	r^2	a	b	b_0	μ_0
		I_1, 60 m (n = 10)			
chl *a*	0.87	0.190	0.0369	0.0609	0.55
chl *b*	0.95	0.080	0.0364	0.0564	0.51
chl *c*	0.96	0.043	0.0512	0.0791	0.71
dv-chl *a*	0.90	0.118	0.0342	0.0441	0.43
Tchl *a*	0.95	0.307	0.0359	0.0547	0.49
		I_1, 30–70 m (n = 11)			
chl *a*	0.84	7.89	0.0266	0.0500	0.56
chl *b*	0.89	3.27	0.0259	0.0501	0.50
chl *c*	0.89	1.79	0.0349	0.0632	0.63
dv-chl *a*	0.88	4.91	0.0230	0.0354	0.35
Tchl *a*	0.90	12.79	0.0253	0.0446	0.45
		I_2, 60 m (n= 9)			
chl *a*	0.81	0.171	0.0336	0.0634	0.51
chl *b*	0.89	0.071	0.0367	0.0682	0.55
chl *c*	0.90	0.040	0.0480	0.0851	0.69
dv-chl *a*	0.84	0.115	0.0454	0.0688	0.55
Tchl *a*	0.90	0.284	0.0392	0.0663	0.53
		I_2, 30–70 m (n = 9)			
chl *a*	0.90	6.61	0.0331	0.0633	0.51
chl *b*	0.89	2.75	0.0338	0.0616	0.49
chl *c*	0.96	1.54	0.0417	0.0769	0.62
dv-chl *a*	0.97	4.70	0.0379	0.0560	0.45
Tchl *a*	0.97	11.29	0.0353	0.0605	0.48

[a]From these regressions, specific growth rate (μo, d^{-1}) and grazing rate (g, d^{-1}) were estimated for each day of the first 48 hours of the time series. At 60 m, D_1 (period from 14 to 5 hours; 4–5 November); I_1 (period from 5 to 14 hours; 5 November); D_2 (period from 14 to 6 hours; 5–6 November); and I_2 (period from 6 to 14 hours; 6 November). Similar periods were also defined for the 30–70 m depth with only slight differences due to depth-related phase shifts (maximum = 1 hour) in the timing of the pigment minima and maxima. Here r^2 = determination coefficient, b_o= b for I_1 and I_2 phases including contemporaneous grazing losses, and n = data number.

[33] Over the full daily cycle, mean grazing rates on FLB correspond to loss rates of 0.64 d^{-1} at 30 m and 0.22 d^{-1} at 60 m. The latter are strongly influenced by one negative estimate during the 2200–0400 time interval, without which the mean rate for the other intervals would be 0.50 d^{-1}. For *Prochlorococcus*, the rate determinations correspond to mortality coefficients of 0.17 d^{-1} at 30 m and 0.22 d^{-1} at 60 m. The latter are similar to the estimate from in situ variations in dv-chl *a* (0.23 d^{-1}) over the same time period (D_1; Table 1). The growth rate estimates for *Prochlorococcus* at both depths also show clear and comparable patterns of cell division within the 1630–2230 time interval (0.11 h^{-1}), with generally negligible growth in the other incubation periods (except later in the night at 30 m). Over the 6-hour duration of these incubations, the daily equivalents rates (0.64–0.65 d^{-1}) are comparable to, and even a little higher than, the full day growth estimates based on pigment increases (Table 1). Unfortunately, while pigment increases during the preceding daylight hours would be the best basis of comparison to the division rates observed at the start of the D_1 phase, we can only compare these results to the pigment estimates during the following day (I_1). Nonetheless, the strong increase in *Prochlorococcus* cell

Table 2. Exponential Regressions $y = ae^{bt}$ of Particulate Organic Carbon (y) as a Function of Time (t) at the Equator (180°)[a]

Period	n	r^2	a	b	b_0	g
			60 m			
D_1	14	0.934	43.16	−0.0203		−0.49
D_2	13	0.884	41.85	−0.0271		−0.65
			30–70 m			
D_1	14	0.927	1874	−0.0244		−0.58
D_2	14	0.977	1861	−0.0291		−0.70
Period	n	r^2	a	b	b_0	μ_0
I_1	12	0.856	32.23	0.0338	0.0541	0.59
I_2	11	0.937	30.08	0.0232	0.0503	0.55
I_1	10	0.95	1383	0.0335	0.0579	0.52
I_2	11	0.905	1258	0.0218	0.0509	0.56

[a]Particulate organic carbon was calculated as c_p^* 500. From these regressions, specific growth rate (μ_o, d^{-1}) and grazing rate (g, d^{-1}) were estimated for each day of the first 48 hours of the time series. At 60 m, D_1 (17 to 7 hours; 4–5 November); I_1 (7 to 16 hours; 5 November); D_2 (16 to 6 hours; 5–6 November); and I_2 (6 to 17 hours; 6 November). Similar periods were also defined for the 30–70 m depth range with only slight differences due to depth-related phase shifts (maximum = 1 hour) in the timing of the c_p minima and maxima. Here r^2 = determination coefficient, b_o = b for I_1 and I_2 phases including contemporaneous grazing losses, and n = data number.

Table 3. Exponential Regressions $y = ae^{bt}$ of in Vivo Tchl *a* Fluorescence (y) as a Function of Time (t) at the Equator (180°)[a]

Period	n	r^2	a	b	b_0	g
			30–70 m			
D1	13	0.993	20.11	−0.0333		−0.80
D2	13	0.926	19.45	−0.0308		−0.74
Period	n	r^2	a	b	b_0	μ_0
			30–70 m			
I_1(a)	7	0.984	13.65	0.0513	0.0846	0.51[b]
I_1(b)	13	0.496	15.00	0.0165	0.0498	0.60
I_2	10	0.927	13.07	0.0291	0.0599	0.76

[a]From these regressions, specific growth rate (μ_o, d^{-1}) and grazing rate (g, d^{-1}) were estimated for each day of the first 48 hours of the time series. D_1 (19 to 7 hours; 4–5 November); I_1 (7 to 13 hours (a) or 19 hours (b); 5 November); D_2 (19 to 7 hours; 5–6 November); and I_2 (7 to 19 hours; 6 November). Here r^2 = determination coefficient, b_o = b for I_1 and I_2 phase including contemporaneous grazing losses, and n= data number.

[b]1.01 for 12-hour extrapolation of the hourly exponential rate.

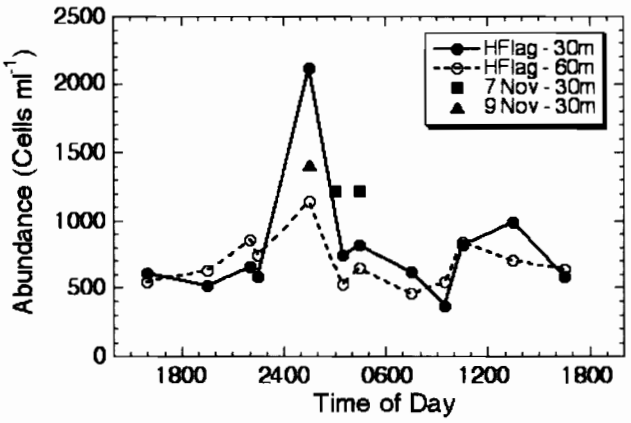

Figure 10. Diel variations in abundance of <20-μm heterotrophic protists at 30 and 60 m. Lines connect the time series of abundance estimates collected during the first day of diel sampling (4–5 November), prior to the arrival of the TIW front. Individual abundance estimates from 7 and 9 November are after the passage of the front.

abundance during the early dark phase both confirms their synchronous pattern of division and suggests that our incubation conditions were not dramatically different from those in the ambient environment.

4. Discussion

[34] Diel variations of in situ chlorophylls and of the chlorophyll cell content have previously been investigated by several authors [*Yentsch and Scagel*, 1958; *Glooschenko et al.*, 1972; *Fuhrman et al.*, 1985] and compiled in different reviews [*Sournia*, 1974; *Harris*, 1978]. To our knowledge, the present study is the first in which diel variations of extracted pigments were studied with high spatiotemporal resolution. Among the most ambitious previous efforts was a 13-day time series with 4 times daily sampling at eight depths in the equatorial Atlantic Ocean [*Le Bouteiller and Herbland*, 1982].

[35] The HNLC zone of the equatorial Pacific is well suited for studies of diel processes based on in situ parameters. Significant and reproducable diel variations in the different chlorophyll concentrations were clear, for example, in the present time series sampling (Figures 3, 4, and 5), providing the basis for dynamical interpretation. In the sections below, we first consider the still unresolved origin of one of the pigments (chl *b*) measured in our study. Subsequently, we discuss the observed diel pigment variations in terms of vertical mixing, physiological and population (growth and grazing) processes, and advection of the TIW.

4.1. Origin of Chlorophyll *b*

[36] The relationships between accessory chlorophylls *b* and *c*, chl *a* and dv-chl *a* were examined to determine the main origin of chl *b*. *Bidigare and Ondrusek* [1996] noted the discrepancy between the relative importance of chl *b* in the central equatorial Pacific and the poor representation of carotenoids associated with chl *b*-containing eukaryotes. They concluded from the known presence of chl *b* in some strains of *Prochlorococcus* [*Partensky et al.*, 1993] that "most of the monovinyl and divinyl chl *b* detected at the EqPac study site originated from *Prochlorococcus* spp.".

[37] During the EBENE time series, HPLC pigment analyses were performed on 30- and 60-m samples in association with dilution experiments [*Landry et al.*, 2003]. As in the analyses of *Bidigare and Ondrusek* [1996], they showed only small concentrations of carotenoids related to known chl *b*–containing eukaryotes. Consequently, they support the notion that the observed concentrations of chl *b* belonged mainly to *Prochlorococcus*. The chl *c*/chl *a* ratios (*c*/*a*) measured by spectrofluorometry were also compatible with this hypothesis. In cultivated chl *c*–containing species, *c*/*a* shows relatively high variation, from 0.04 to 0.3 [*Vesk and Jeffrey*, 1987]. If we assume a mean *c*/*a* value of 0.1 or 0.2 for our samples, there appears to be insufficient chl *a* to obtain chl *b*/chl *a* ratios compatible with those observed in chl *b*–containing algal cultures. For a *c*/*a* ratio of 0.3, the *b*/*a* ratios in surface samples were often unreasonably high (range: 0.54–2.08). Some high chl *b*/dv-chl *a* ecotypes [see *Moore and Chisholm*, 1999] of *Prochlorococcus* are known to synthetize chl *b* under relatively high light irradiance [*Moore et al.*, 1995], and a sizable part of chl *b* could be due to *Prochlorococcus*. The high ratio of chl *b*/dv-chl *a* agrees with this hypothesis (>0.33), but the high variation of this ratio (0.33 to 0.89) suggests the presence of another algal population rich in chl *b* near the surface.

[38] In addition, the linear correlation coefficient (r) between dv-chl *a* and chl *b* in surface samples was low 0.39 (n = 65) compared to that between chl *a* and chl *b* (0.88) or between chl *c* and chl *b* (0.96: Figure 11a). The strong relationship between chl *b* and chl *c* is particularly surprising if one assumes that the two pigments are generally not present in the same cells. Moreover, the negative correlation of the chl *b*/dv-chl *a* ratio with the percentage of dv-chl *a* (Figure 11b; r = −0.84) is opposite to what might be expected if chl *b* is mainly associated with *Prochlorococcus*, unless different populations of *Prochlorococcus* were present in various proportions during the time series. Flow cytometry did not indicate the occurrence of different populations, as would be evident in cellular fluorescence properties. Furthermore, some in situ incubations of surface samples during the light period showed a dramatic decrease of the dv-chl *a* concentration, but not chl *b* (chl *b*/dv-chl *a* ratio ≈ 3).

[39] Methodological problems can occur in the estimation of the accessory chlorophylls if some are not taken into account in the spectrofluorometric analyses. Such is the case for chlorophyll *c3* which was first observed in *Pelagococcus*

Table 4. Rate Estimates (g = grazing rate; μ = specific growth rate) From Size-Fractioned Incubation Experiments Conducted in 6-Hour Time Intervals Over a Diel Cycle[a]

	30 m			60 m		
Time	FLB	*Prochlorococcus*		FLB	*Prochlorococcus*	
Interval	g, h^{-1}	μ, h^{-1}	g, h^{-1}	g, h^{-1}	μ, h^{-1}	g, h^{-1}
1630–2230	0.015	0.109	0.015	0.022	0.107	0.011
2200–0420	0.032	0.042	0.013	−0.027	0.006	0.001
0400–1010	0.030	0.002	0.004	0.023	0.002	0.011
1100–1700	0.030	−0.012	−0.002	0.018	0.008	0.013

[a]Seawater collected at 30 and 60 m. Rate determinations for fluorescently labeled bacteria (FLB) and *Prochlorococcus* spp. as indicated in section 2.6.

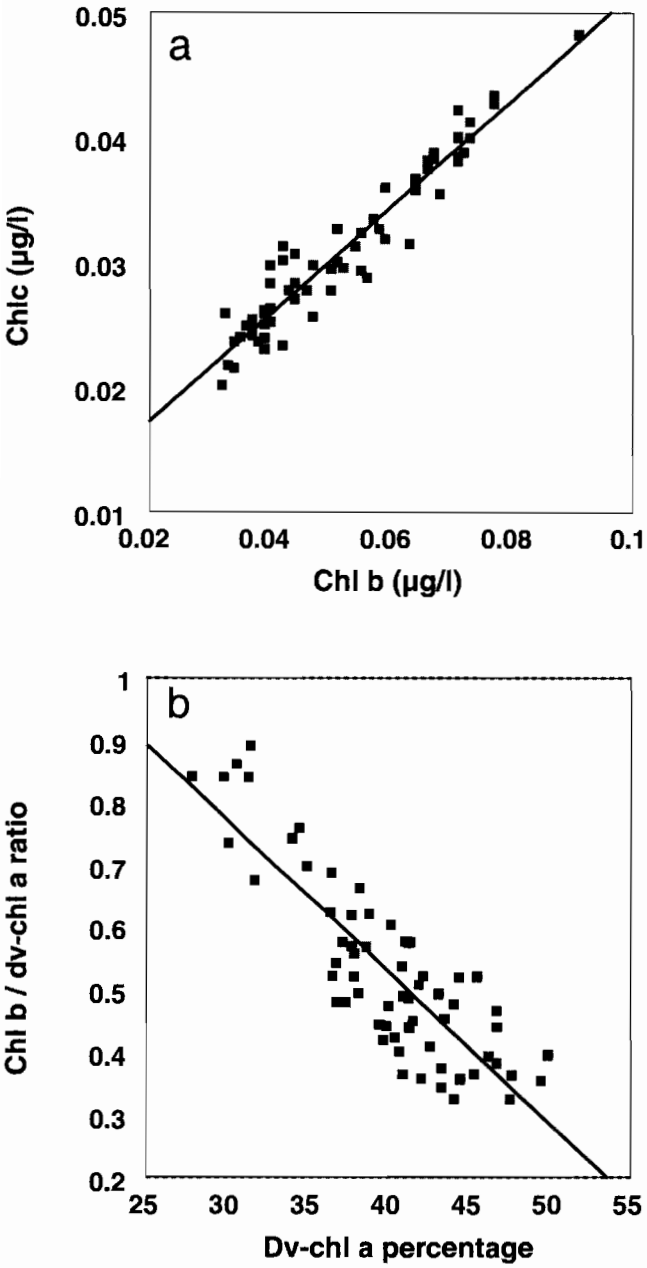

Figure 11. Diel variations at 0 m during the 5-day time series at the equator (180°). Linear regression of (a) chl *c* versus chl *b* and (b) chl *b*/dv-chl *a* ratio versus dv-chl *a* percentage.

subviridis [*Vesk and Jeffrey*, 1987] and *Emiliana huxleyi* [*Jeffrey and Wright*, 1987]. This pigment has slight differences in its spectral properties compared to chlorophylls *c1* and *c2*. Recently, chl *c3* was resolved into two components in *Emiliana huxleyi* [*Garrido et al.*, 1995]. HPLC analyses on 30- and 60-m samples showed the existence of chl *c3* in the proportion of 40–45% of the total chl *c* (*c*1 + *c*2 + *c*3) and similar concentration for chl *c*1 + chl *c*2 than spectrofluorometric measurements. The addition of chl *c*3 measured by HPLC lead to total chl *c*/chl *a* ratio of 0.33–0.38. Recently, high total chl *c*/chl *a* ratio was reported in cultures of *Chrysochromulina* species (Haptophyta), between 0.38 to 0.60 [*Zapata et al.*, 2001]. The presence of a relatively high concentration of 19′-Hexanoyloxyfucoxanthin suggested that Haptophyceae algae were major components of the community in our samples. Thus the presence of species containing high total chl *c*/chl *a* would allow us to attribute chl *b* at least partly to eukaryotic algae and explain the important variation of the chl *b*/dv-chl *a* ratio in the near-surface time series. Another spectrally distinct pigment related to the chl *c* family, the Mg-3-8 D, is present with chl *b* in some Prasinophyceae [*Ricketts*, 1966] and some strains of *Prochlorococcus marinus* [*Goericke and Repeta*, 1993; *Goericke et al.*, 2000]. However, in these organisms, the concentration of Mg-3-8 D is weak compared to that of chl *b*. The inclusion of a standard for Mg 3-8 D in the spectrofluorometric analyses showed that this pigment was not a significant component in our samples and could not have influenced seriously the accessory chlorophyll estimates. Spectrofluorometric analyses of size-fractionated samples could help to solve this question. Unfortunately, the one set of size-fractionated samples from EBENE were filtered too coarsely (10-, 5-, and 3-µm Nuclepore filters and Whatman GF/F). The results showed that 70% of chl *b* was associated with the <3-µm fraction, but did not allow us to distinguish whether the pigment was associated with prokaryotes (<1 µm) or tiny eukaryotic cells. Given all of the contradictory evidence discussed above, perhaps some unique populations still remain to be discovered.

4.2. Overview of Diel Parameter Variations

[40] At a given depth of a fixed station, the variations in pigment concentrations are the result of various factors including: 1) the balance between growth and mortality of phytoplankton, 2) cellular physiological responses to environmental modifications (e.g., photoacclimation to the light field), and 3) the effects of external physical factors such as vertical mixing, internal waves, advection and sinking. During the time series at the equator, the advection of a relatively fresh, warm and nitrate-poor water mass could have influenced abundance, structure and functionning of the biological community and consequently timing and amplitude of diel variations. This water mass which seemed link to the southward branch of a Tropical Instability Wave (TIW) [*Eldin and Rodier*, 2003] reached the surface layer at our station 24 hours after the beginning of time series sampling and slightly later (1–4 hours) in the 30–70 m layer. So, it would not have affected diel variations during the D_1 and I_1 phases as defined in Material and Methods (section 2.5.) or μ_o and g estimates at 60 m and in the 30–70 m range. The passage of the front occurred during D_2. Surprisingly, it did not strongly affect the ISCV and c_p variations in the 30–70 m layer, but could be the reason for the double peak structure of F_{iv} at the end of I_1, as well as the enhanced grazing rate estimates from diel chl *a*, chl *b*, chl *c* and c_p variations when the lower chlorophyll waters were advected in the study area.

[41] Since physical factors that create stability (heat) prevail during the daytime, the increasing water column stability during the first part of the light period should reduce the vertical displacement of cells and tend to maintain them within more restricted depth ranges [*Farmer and MacNeil*, 1999]. Thus changes during the I phases could be more indicative of net growth rate than the D phases of the grazing rates, particularly when vertical mixing increases during the night.

[42] In the upper mixed layer, photoacclimation to high light is expected to alter cellular chl *a* concentration independently of cell growth and mortality. Deeper in the euphotic zone, pigments should increase with cell growth during the daylight period and decrease during the night because of grazing activity. This is well illustrated by the diel variations of integrated pigment concentrations, in vivo fluorescence and c_p in the 30–70 m layer. However, slight differences occurred in timing of the minima and maxima of the different parameters. Generally, the Tchl *a* minima and maxima preceded those for c_p and F_{iv}. Moreover, assuming a direct relationship between c_p and POC, the POC/Tchl *a* ratio showed broad maxima and minima with sharp transitions in the later part of the night and in the afternoon. The broad minima correspond mainly to the I periods for Tchl *a* (0800–1400 hours) and could reflect a time of balanced growth for carbon and Tchl *a*. Thereafter, chlorophyll synthesis would occur only to maintain a nearly constant pigment pool in the cell (turnover), while carbon would continue to accumulate by photosynthesis, increasing the POC/Tchl *a* ratio until sunset. This increase could be the effect of cell cycle metabolism associated with DNA synthesis preceding nocturnal cell division. For example, *Vaulot et al.* [1995] reported most *Prochlorococcus* cells in the DNA synthesis phase during the afternoon. The sharp decrease in the ratio at the end of the night can be partly explained by unbalanced growth between 0500 and 0800 hours, since chlorophyll synthesis seemed to start just before sunrise and the minimum of Tchl *a* occurred 1–2 hours before that of c_p. In the 0–30 m layer, the situation was different since most of the increase in Tchl *a* was nocturnal with a peak in early morning (0900 hours). In addition, the 0–30 m increase in integrated F_{iv} occurred from noon to sunset, and that of integrated c_p was also limited to the light period. Most often, integrated F_{iv} was negatively correlated ($p < 0.01$) with extracted Tchl *a*, as for example during the increase phase of integrated Tchl *a*, from 2100 to 0900 hours on 4–5 November ($r = -0.967$, $n = 13$). Thus the use of the F_{iv} signal to assess variations of extracted Tchl *a* in the 0–30 m layer appears problematic.

[43] During EBENE, attempts to estimate μ_0 and g in the 30–70 m depth range appear theoretically justified whatever the parameter used (integrated c_p, Tchl *a* and F_{iv}), since the increases coincided with energy (light) input in the ecosystem. However, in the 0–30 m layer, integrated Tchl *a* and F_{iv} exhibit relatively independent diel variations from each other and from c_p (Figures 7a and 8a). In this layer, the F_{iv} signal is strongly influenced by physiological responses of cells (independent of growth and chlorophyll concentration) to high illumination during the light period, including photochemical quenching, which peaks at noon [*Kiefer*, 1973]. Exponential regression on the I phases (from noon to 2100 hours) would lead to μ_0 estimates of around 1.3 (approximately 2 divisions d^{-1}), clearly higher than estimates obtained from c_p. The increasing phase of Tchl *a* does not appear to be associated with cell growth, except in the early morning (see section 4.3.). It seems rather influenced by two factors: vertical mixing and cellular chlorophyll synthesis, partially photobleaching during high daytime illumination. Considering the first day of the time series, nocturnal vertical mixing affected a layer greater than 30-m thickness, which can lead to a decline of pigments in the deep chlorophyll maximum layer and an enrichment in the 0–30 m layer. However, when nocturnal vertical mixing was limited to the upper 30 m during the other days of the time series, the increase seemed more related to chlorophyll synthesis. Paradoxically, the relative increase of integrated Tchl *a* was not strongly different between the first and the following days. The decreasing phase of integrated Tchl *a* reflected both grazing and cellular pigment decrease related to high light. However, between 0900 hours and midnight on 5 November, it showed a greater amplitude than usual as the result of the advective influence of the TIW.

[44] Diel variations of Tchl *a* were similar to those observed previously in the equatorial Atlantic Ocean (CIPREA cruise) with a maximum around 1400 hours at 60-m depth [*Le Bouteiller and Herbland*, 1982]. Contrary to the present study, however, the maximum of Tchl *a* occurred around 1400 hours from 0 to 80 m. This difference can be explained by the more intense vertical stratification in the Atlantic during the CIPREA cruise than in the Pacific during EBENE. High stratification would maintain cells at relatively constant depth with the result that they would be fully photoacclimated from one day to another at their residence light level [*Le Bouteiller et al.*, 2003].

4.3. Phytoplankton Growth and Zooplankton Grazing Rates

[45] Several methods have been applied to determining the rates of phytoplankton growth and microzooplankton grazing in the upwelling region of the equatorial Pacific. Some use incubation procedures and biomass estimators, such as dilution [*Chavez et al.*, 1991; *Verity et al.*, 1996; *Landry et al.*, 1995] or ^{14}C uptake [*Chavez et al.*, 1996; *Landry et al.*, 1997]. Others use high-frequency vertical profiles of particle light attenuation [*Siegel et al.*, 1989; *Claustre et al.*, 1999], cell abundances [*Blanchot et al.*, 1997; *André et al.*, 1999], or cell cycle analyses from DNA staining [*Vaulot et al.*, 1995; *Vaulot and Marie*, 1999]. Most of these methods give specific growth rates around 0.6–0.7 d^{-1} at the surface and maximum values of 0.8–1.0 d^{-1}.

[46] In addition to the present study, phytoplankton growth and microzooplankton grazing rates were also determined during the EBENE cruise from dilution experiments based on spectrofluorometric and HPLC pigment analyses, as well as flow cytometric (FCM) cell counts [*Landry et al.*, 2003]. For a given sampling date, growth rate estimates from these experiments were higher under conditions simulating the 30-m light level compared to those for 60 m (e.g., 0.90 versus 0.29 d^{-1} for mean estimates based on Tchl *a*, and 0.61 versus 0.26 d^{-1} for dv-chl *a*). In comparison, growth estimates from 30–70 m integrated in situ chlorophyll variation (ISCV) revealed little depth structure and tended to be intermediate (e.g., 0.45–0.53 d^{-1} for Tchl *a* and 0.35–0.55 d^{-1} for dv-chl *a*; Table 1) between experimental estimates at the two fixed depth light levels. Thus there was a relatively good agreement between experimental and ISCV approaches with respect to mean growth rates over the 30–70 m depth interval, but the in situ community appeared to experience a more uniform light field than the bottle incubated samples.

[47] Since ISCV grazing rate inferences were also based on the magnitudes of daily oscillations, it follows that they would be similarly affected by the physical or physiological

processes that smeared the depth distribution of the growth signal. For Tchl *a*, the experimentally derived grazing coefficients at the equator ranged from 0.52 to 0.73 d^{-1} (mean = 0.64 d^{-1}) at 30 m and 0.11 to 0.24 d^{-1} (mean = 0.18 d^{-1}) at 60 m, compared to in situ estimates of 0.42 to 0.65 d^{-1} (mean = 0.53 d^{-1}). These estimates are in excellent agreement if we add an additional ~0.1 d^{-1} to the experimental estimates of microzooplankton grazing to account for the grazing contribution of mesozooplankton in the ambient environment [*Champalbert et al.*, 2003]. For smaller phytoplankton such as *Prochlorococcus*, we can reasonably expect that the microzooplankton grazing rates, measured either by dv-chl *a* or FCM cell counts, would represent all of the community grazing impact. Experimental estimates for grazing on *Prochlorococcus* ranged from 0.51 to 0.84 d^{-1} (mean = 0.62 d^{-1}) at 30 m and 0.20 to 0.43 d^{-1} (mean = 0.27 d^{-1}) at 60 m. The ISCV estimates (0.23–0.57 d^{-1}; mean = 0.38 d^{-1}) are clearly consistent with these experimental determinations.

[48] Rate estimates from our ISCV analyses are based on the assumption that grazing rates were more-or-less constant over the 24-hour cycle. The supporting data are equivocal. On one hand, neither the short-term grazing experiments with *Prochlorococcus* nor the diel sampling of protistan grazer abundance revealed significant day-night differences that would invalidate this assumption. On the other hand, we have some indication that peak abundances of heterotrophic protists may occur during the night. If this is indeed the case, then the diel cycle of protistan grazers in the equatorial Pacific is opposite to that observed (midday maximum) off coastal California [*Fuhrman et al.*, 1985]. In addition, higher protist densities in the nighttime would add to rather than offset the diel cycle for mesozooplankton in the euphotic zone. In considering the implications of these cycles for grazing impacts, it is important to note that higher abundance or biomass do not necessarily equate to higher grazing activity. For example, concentrated cell division of heterotrophic protists during the night might come at the expense of time spent feeding. Moreover, the higher biomass of mesozooplankton in nighttime sampling may not reflect more grazing if many or most of the migrating taxa feed carnivorously. This may in fact be the case at the EBENE equatorial time series station, where *Champalbert et al.* [2003] found insignificant differences in community gut fluorescence (the product of biomass-specific gut fluorescence and mesozooplankton biomass) for day and nighttime sampling. We therefore acknowledge the likelihood that grazing occurs somewhat unevenly over the daily cycle, but within broadly defined day and nightime periods the differences seem to be relatively small.

[49] In contrast, *Claustre et al.* [1999] inferred grazing rates twofold higher during the night than during the light period from diel integrated c_p variations in the equatorial Pacific. As noted by *Claustre et al.* [1999], part of the explanation for this apparent result could be the effect of other biological and physical processes (aggregation, mixing and growth of heterotroph populations) on the diel c_p signal. However, their rate calculations for μ, computed as double the net increase observed during the light period, also appear to have been in error. Intuitively, one would not double the net light period rate if the grazing rate in the light was substantially less than that in the dark. The "correction" for daylight grazing losses would be lower. Moreover, most of the data in both the present study and *Claustre et al.* [1999] show the growth phase of the c_p diel signal to be substantially less than the 12 hours assumed. Thus their observations are largely consistent with the present findings in which positive net growth over a <12-hour period is balanced by lower and relatively constant rates of grazing losses over the full day.

4.4. Photoacclimation Effects on Rate Estimates

[50] Under fixed environmental conditions, all major chemical components should increase similarly during cell growth in order to be maintained in similar proportion, at least at the same phase of the cell cycle (= balance growth) [*Cullen and Lewis*, 1988]. It is well known that light transitions can lead to unbalanced growth and modifications in cellular C/chl *a* ratio and chl *a* content (photoacclimation). Transitions from high to low light are followed by increasing cellular chl *a* content (a decrease in C/chl *a* ratio), and the opposite occurs for transitions from low to high light [*Falkowski*, 1984; *Post et al.*, 1984, 1985; *Cullen and Lewis*, 1988]. In previous studies, first-order kinetics reasonably described the photoacclimation process in different algal cultures [*Falkowski*, 1984; *Post et al.*, 1984, 1985] and in the context of vertical mixing [*Cullen and Lewis*, 1988]. In the present study, variations occur with respect to both photocycle at a given sampling depth as well as vertical cell displacements from different depths in the water column. Thus the important question is whether the cells were photoacclimated to light levels at the depth of sampling.

[51] On the basis of analyses of photosynthesis light curves at 0°, 150°W, *Cullen et al.* [1992] concluded that the phytoplankton appeared well adapted to ambient light fluctuations in the equatorial Pacific upwelling regime. However, their experiments occurred under conditions of greater vertical stratification than the present time series. At the equator during EBENE, mixed layer depth (Z_m = depth where the density gradient exceeds 0.01 kg m^{-4}) [*Lukas and Lindstrom*, 1991] was always located between 80 and 110 m. For the EqPac cruises, *Gardner et al.* [1995] used Z_m defined by the depth of an increase of 0.03 kg m^{-3} relative to surface density. With this latter definition, Z_m during EBENE varied more dynamically from 10 to 70 m. Temperature profiles showed a shallow diurnal thermocline (10–20 m) related to solar heating being disrupted by nocturnal mixing. Using the coefficient of variation of σ_θ (CV_d), it was possible to see more finely the relative stratification and vertical mixing in the mixed layer. During the first 24 hours of observation, destratification began in the afternoon and mixing of the water column extended to approximately 60 m by the end of the night (Figure 2). In the following days, complete nocturnal mixing occurred only in the first 20–30 m. In the 30–70 m layer, CV_d variations indicated a transition to more stratified waters, related to advective flow of the TIW [*Eldin and Rodier*, 2003], which remained until the end of the sampling period and was not tightly coupled with the day-night cycle. The vertical distribution of Tchl *a* was quasi homogeneous to 80-m depth at the end of the D_1 phase, when the vertical mixing was more intense. However, the abundance of the three picoplankton populations (*Synechococcus*, *Prochlorococcus* and picoeukaryotes), which represented about 70%

of Tchl *a* (according to 3-μm size fractionation of pigments), was homogeneous only in the upper 30–40 m (i.e., in a layer where density varied by 0.01 kg m^{-3}), decreasing slightly with depth [*Blanchot et al.*, 2003]. Moreover, the red fluorescence *per* cell increased with depth in the 30–70 m layer. If we assume therefore that cells below 30 m (40 m on the first day) were largely photoacclimated to the depth of sampling, ISCV variations in the 30–70 m depth range during the I_1 phase should have reflected balanced growth. Consistent with this view, the cellular forward light scatter (an index of cell size) and cellular red fluorescence (an index of chl concentration) both approximately doubled (1.8–2.0) during the I_1 phase at 60 m. In addition, while stratification was more pronounced during I_2, ISCV gave similar estimates of μ_0 (0.5–0.55 d^{-1}).

[52] For the diatom *Thalassiosira weisflogii* on a 12h:12h artificial light:dark cycle, *Post et al.* [1984] showed that the maximum chl *a* $cell^{-1}$ occurred 8 hours after the onset of illumination and then decreased. This result is similar to our field observations. The variations of chl *a* $cell^{-1}$ were not correlated with cell division in *T. weisflogii*, which was only partially synchronized under culture conditions [*Post et al.*, 1984]. However, similar results were obtained for an asynchronously dividing culture of *Skeletonema costatum* [*Owens et al.*, 1980].

[53] It is difficult to assess how much of the observed ISCV at 30–70 m could be due to decreasing chl *a* $cell^{-1}$ during the D phase independent of cell division. This influence could lead to an overestimate of g and consequently of μ_0. In vivo chl fluorescence $cell^{-1}$ as measured by flow cytometry gives an estimate of chlorophyll content of picoplanktonic cells. However, in vivo chl *a* fluorescence responds both to chl *a* concentration and to physiological modifications in the structure and functioning of the photosynthetic apparatus. In vivo fluorescence in the 30–70 m depth range continued to increase until the end of the afternoon (1900 hours) while Tchl *a* concentration decreased earlier. Finally, the highest μ_0 was observed from chl *c* estimates, suggesting a faster growth rate for chl *c*–containing eukaryotes, and leading to an increased chl *c*/chl *a* ratio. For this, however, we cannot completely exclude photoacclimation effects, since chl *c*/chl *a* ratios can increase slightly when cells are transferred from high to low light [*Post et al.*, 1985]. This effect will be related to the previous light history of the cell and not to ambient light since the increase of the chl *c*/chl *a* ratio in our time series occurred when ambient light increased.

[54] In the upper 30 m of the water column, a diurnal thermocline tended to maintain the phytoplankton community at strong solar illumination. In sampling within this depth range, Tchl *a* concentration increased during the night, from around midnight to early in the morning, then it decreased until the next midnight. Part of this increase was likely related to vertical mixing during the first night, but may have also been associated with increased chlorophyll per cell during the other nights. However, the relative increase was more important for dv-chl *a* than for chl *a*. Red fluorescence of *Prochlorococcus* cells increased during the second part of the night, just after cell division [*Vaulot and Marie*, 1999; J. Blanchot et al., unpublished manuscript], suggesting a possible synthesis of dv-chl *a* and an increase of dv-chl *a* $cell^{-1}$. This synthesis could explain the relative increase of the dv-chl *a* percentage observed during this period. Mean red fluorescence of *Synechococcus* and picoeukaryotes also increased in the dark (J. Blanchot et al., unpublished manuscript). Diel variations of the total fluorescence of the three picoplanktonic populations (F_{pico}), measured as $\sum_{i=1}^{i=3} F_i^* N_i$ (F = red fluorescence *per* cell; N = cell number) matched better with variations in Tchl *a* than F_{iv}. This difference can be explained by the fact that F_{iv} represents the instantaneous state of the photosynthetic systems whereas F_{pico} was assessed after a relatively long dark period (1–2 hours) which modified this state. Forward Scattering (Fs), the flow cytometric index of cell size, indicated that the nocturnal increase of integrated Tchl *a* was not related to cell growth. Integrated Tchl *a* increased while Fs remained stable during the second half of the night for *Prochlorococcus* and picoeukaryotes, the main contributors to picoplankton Tchl *a* (Figure 12). For *Synechococcus*, Fs generally increased (except on the first night) but slower than integrated Tchl *a*. Consequently, the rate estimates of μ_0 and g from ISCV were problematic for the upper mixed layer. Nevertheless, the amplitudes of the variations in integrated Tchl *a* between 2300 and 0900 hours for 4 and 5 November are similar to the increase of integrated c_p during the light period (0600 to 1600 hours, 5 November), implying comparable growth rates.

5. Conclusions

[55] The HNLC region of the equatorial Pacific is an attractive area for studying and modeling the biological process relationships from high-frequency sampling. In the present study, spectrofluorometric pigment analysis and picoplankton characterization by flow cytometry at hourly frequency provided useful complements to the more automated continuous profiles of F_{iv} and c_p. Our results demonstrate the dynamical and synchronized growth of phytoplankton at the equator and the near-perfect balance between daily growth increases and grazing losses. At depths extending from 30 to 70 m (10 to 1% of surface PAR), diel variations of pigment concentrations, F_{iv} and c_p were relatively similar showing an increasing phase (I) during the daily light period and a decreasing phase (D) at night. Only some differences occurred in the durations of each phase and in the timings of the minima and especially the maxima, which appeared sooner for Tchl *a* than for c_p and F_{iv}. From in situ variations of c_p, a simple growth-grazing model gave mean μ_0 and g estimates of 0.54 and 0.64 d^{-1} which were intermediate between those determined from Tchl *a* (0.47 and 0.51 d^{-1}) and those obtained from F_{iv} (0.68 and 0.77 d^{-1}). Higher values of μ_0 and g were calculated from chl *a* than from dv-chl *a* variations suggesting a more dynamic role for eukaryotes and their grazers. The accuracy of derived μ_0 and g estimates from in situ variations depends on the assessment of the minima, maxima and phase durations as well as the validity of assumptions regarding the relationships of these phases to growth and grazing processes under ideal circumstances. In addition, one needs to sample a single water mass characterized by horizontally homogeneous distributions of pigment, c_p or F_{iv}. In the present study, the passage of a TIW after the first sampling day did not seem to have markedly

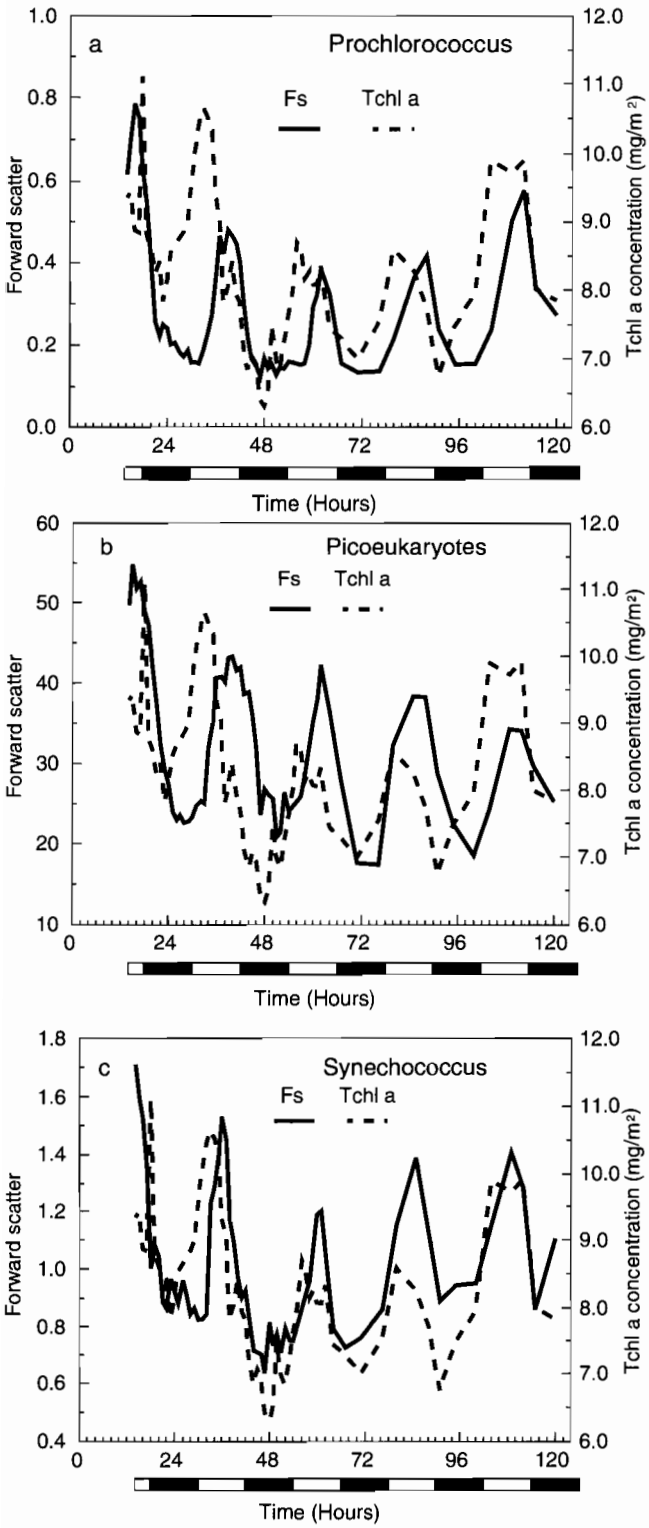

Figure 12. Diel variations of integrated cellular forward scatter, in the 0–30 m layer of (a) *Prochlorococcus*, (b) picoeukaryotes, and (c) *Synechococcus* during the 5-day time series at the equator. Comparison with diel variations of integrated total chlorophyll *a* (dashed line).

affected pigment and c_p variations in the 30–70 m layer but may have led to exaggerated grazing rate estimates during the water mass transition. In the 0–30 m layer (100 to 10% of surface PAR), it was also possible to divide daily variations into I and D phases. However, the patterns for integrated c_p, F_{iv} and Tchl *a* variations were clearly out of phase. The variations of integrated c_p were similar to those in the underlying layer with an increase during the light period. In contrast, the increase of Tchl *a* was essentially nocturnal while F_{iv} increased during the afternoon and the evening. Generally, F_{iv} variations were not correlated with extracted Tchl *a*, so the assessment of Tchl *a* from F_{iv} in the 0–30 m layer is an interesting problem for future studies of light and timing effects.

[56] **Acknowledgments.** We are particularly indebted to Rick Miller (PMEL, Seattle), Timothy Nesseth (PMEL, Seattle) and Alain Lapetite (IRD, Nouméa) who efficiently helped us in the tedious and boring filtration and pigment extraction tasks during the time series. Without them hourly sampling at ten depths with subsequent pigment analysis on board would have been impossible. Thanks to Francis Gallois and Jean-Yves Panché for their efficient work in hydrological data acquisition. In particular, we thank Robert Le Borgne (IRD, Nouméa) for his superb efforts in organizing and leading the EBENE cruise. We thank Denis MacKey (CSIRO, Hobart) and an anonymous reviewer for their helpful criticisms. This work was supported by CNRS-INSU, UMR 7621 and IRD.

References

André, J. M., C. Navarette, J. Blanchot, and M.-H. Radenac, Picophytoplankton dynamics in the equatorial Pacific: Growth and grazing rates from cytometric counts, *J. Geophys. Res.*, *104*, 3369–3380, 1999.

Bidigare, R. R., and M. Ondrusek, Spatial and temporal variability of phytoplankton pigment distributions in the central equatorial Pacific Ocean, *Deep Sea Res., Part II*, *43*, 809–833, 1996.

Bishop, J. K. B., Transmissometer measurement of POC, *Deep Sea Res., Part I*, *46*, 353–369, 1999.

Blanchot, J., and M. Rodier, Picophytoplankton abundance and biomass in the western tropical Pacific Ocean during the 1992 El Niño year: Results from flow cytometry, *Deep Sea Res., Part I*, *43*, 877–895, 1996.

Blanchot, J., J.-M. André, C. Navarette, and J. Neveux, Picophytoplankton dynamics in the equatorial Pacific: Diel cycling from flow-cytometer observations, *C. R. Acad. Sci.*, *320*, 925–931, 1997.

Brown, S. L., M. R. Landry, J. Neveux, and C. Dupouy, Microbial community abundance and biomass along a 180° transect in the equatorial Pacific during an El Niño-Southern Oscillation cold phase, *J. Geophys. Res.*, *108*(C12), 8139, doi:10.1029/2001JC000817, in press, 2003.

Calbet, A., and M. R. Landry, Mesozooplankton influences on the microbial food web: Direct and indirect trophic interactions in the oligotrophic ocean, *Limnol. Oceanogr.*, *44*, 1370–1380, 1999.

Champalbert, G., J. Neveux, R. Gaudy, and R. Le Borgne, Diel variations of copepod feeding and grazing impact in the high-nutrient, low-chlorophyll zone of the equatorial Pacific Ocean (0°; 3°S, 180°), *J. Geophys. Res.*, *108*(C12), 8145, doi:10.1029/2001JC000810, in press, 2003.

Chavez, F. P., K. R. Buck, K. H. Coale, J. H. Martin, G. R. DiTullio, N. A. Welschmeyer, A. C. Jacobson, and R. T. Barber, Growth rates, grazing, sinking, and iron limitation of equatorial Pacific phytoplankton, *Limnol. Oceanogr.*, *36*, 1816–1833, 1991.

Chavez, F. P., K. R. Buck, S. K. Service, J. Newton, and R. T. Barber, Phytoplankton variability in the central and eastern tropical Pacific, *Deep Sea Res., Part II*, *43*, 835–870, 1996.

Claustre, H., A. Morel, M. Babin, C. Caillau, D. Marie, J. C. Marty, D. Tailliez, and D. Vaulot, Variability in particle attenuation and chlorophyll fluorescence in the tropical Pacific: Scales, patterns and biogeochemical implications, *J. Geophys. Res.*, *104*, 3401–3422, 1999.

Cullen, J. J., and M. R. Lewis, The kinetics of algal photoadaptation in the context of vertical mixing, *J. Plankton Res.*, *10*, 1039–1063, 1988.

Cullen, J. J., M. R. Lewis, C. O. Davis, and R. T. Barber, Photosynthetic characteristics and estimated growth rates indicate grazing is the proximate control of primary production in the equatorial Pacific, *J. Geophys. Res.*, *97*, 639–654, 1992.

Dandonneau, Y., and J. Neveux, Diel variations of in vivo fluorescence in the eastern equatorial Pacific: An unvarying pattern, *Deep Sea Res., Part II*, *44*, 1869–1880, 1995.

Dunne, J. P., J. W. Murray, J. Young, L. S. Balestrieri, and J. Bishop, ^{234}Th and particle cycling in the central equatorial Pacific, *Deep Sea Res., Part II*, *44*, 2049–2083, 1997.

Durand, M. D., and R. J. Olson, Contributions of phytoplankton light scattering and cell concentration changes to diel variations in beam attenuation in the equatorial Pacific from flow cytometric measurements of pico-, ultra- and nanoplankton, *Deep Sea Res., Part II, 43*, 891–906, 1996.

Eldin, G., and M. Rodier, Ocean physics and nutrient fields along 180° during an El Niño-Southern Oscillation cold phase, *J. Geophys. Res., 108*(C12),8137, doi:10.1029/2000JC000746, in press, 2003.

Falkowski, P. G., Kinetics of adaptation to irradiance in *Dunaliella tertiolecta*, *Photosynthetica, 18*, 62–68, 1984.

Farmer, D., and C. McNeil, Photoadaptation in a convective layer, *Deep Sea Res., Part II, 46*, 2443–2446, 1999.

Fuhrman, J. A., R. W. Eppley, A. Hagström, and F. Azam, Diel variations in bacterioplankton, phytoplankton, and related parameters in the Southern California Bight, *Mar. Ecol. Prog. Ser., 27*, 9–20, 1985.

Gardner, W. D., S. P. Chung, M. J. Richardson, and I. D. Walsh, The oceanic mixed-layer pump, *Deep Sea Res., Part II, 42*, 757–775, 1995.

Garrido, J. L., M. Zapata, and S. Muñiz, Spectral characterization of new chlorophyll *c* pigments isolated from *Emiliana huxleyi* (Prymnesiophyceae) by high-performance liquid chromatography, *J. Phycol., 31*, 761–768, 1995.

Glooschenko, W. A., H. Curl Jr., and L. F. Small, Diel periodicity of chl *a* concentration in Oregon coastal waters, *J. Fish. Res. Board Can., 29*, 1253–1259, 1972.

Goericke, R., and D. J. Repeta, Chlorophylls *a* and *b* and divinyl chlorophylls *a* and *b* in the open subtropical North Atlantic Ocean, *Mar. Ecol. Prog. Ser., 101*, 307–313, 1993.

Goericke, R., R. J. Olson, and A. Shalapyonok, A novel niche for *Prochlorococcus* sp. in low-light suboxic environments in the Arabian Sea and the eastern tropical North Atlantic, *Deep Sea Res., Part I, 47*, 1183–1205, 2000.

Harris, G. P., Photosynthesis, productivity and growth: The physiological ecology of phytoplankton, *Arch. Hydrobiol., 10*, 1–171, 1978.

Jeffrey, S. W., and S. W. Wright, A new spectrally distinct component in preparation of chlorophyll c from the microalga *Emiliana huxleyi* (Prymnesiophyceae), *Biochim. Biophys. Acta, 894*, 180–188, 1987.

Kiefer, D. A., Chlorophyll *a* fluorescence in marine centric diatoms: Responses of chloroplasts to light and nutrient stress, *Mar. Biol., 23*, 39–46, 1973.

Landry, M. R., J. Constantinou, and J. Kirshtein, Microzooplankton grazing in the central equatorial Pacific during February and August, 1992, *Deep Sea Res., Part II, 42*, 657–672, 1995.

Landry, M. R., et al., Iron and grazing constraints on primary production in the central equatorial Pacific: An EqPac synthesis, *Limnol. Oceanogr., 42*, 405–418, 1997.

Landry, M. R., S. L. Brown, J. Neveux, C. Dupouy, J. Blanchot, S. Christensen, and R. R. Bidigare, Phytoplankton growth and microzooplankton grazing in high-nutrient, low-chlorophyll waters of the equatorial Pacific: Community and taxon-specific rate assessments from pigment and flow cytometric analyses, *J. Geophys. Res., 108*(C12),8142, doi:10.1029/2000JC000744, in press, 2003.

Laws, E. A., G. R. DiTullio, K. L. Carder, P. R. Betzer, and S. Hawes, Primary production in the deep blue sea, *Deep Sea Res., Part A, 37*, 715–730, 1990.

Le Borgne, R., and M. Rodier, Net zooplankton and the biological pump: A comparison between the oligotrophic and mesotrophic equatorial Pacific, *Deep Sea Res., Part II, 44*, 2003–2023, 1997.

Le Borgne, R., M. Rodier, A. Le Bouteiller, and J. W. Murray, Zonal variability of plankton and particle export flux in the equatorial Pacific upwelling between 165°E and 150°W, *Oceanol. Acta, 22*, 57–66, 1999.

Le Borgne, R., G. Champalbert, and R. Gaudy, Mesozooplankton biomass and composition in the equatorial Pacific along 180°, *J. Geophys. Res., 108*(C12), 8143, doi:10.1029/2000JC000745, 2003.

Le Bouteiller, A., and A. Herbland, Diel variation of chlorophyll *a* as evidenced from a 13-day station in the equatorial Atlantic Ocean, *Oceanol. Acta, 5*, 433–441, 1982.

Le Bouteiller, A., J. Blanchot, and M. Rodier, Size distribution patterns of phytoplankton in the western Pacific: Towards a generalization for the tropical open ocean, *Deep Sea Res., Part A, 39*, 805–823, 1992.

Le Bouteiller, A., A. Leynaert, M. Landry, R. Le Borgne, J. Neveux, M. Rodier, J. Blanchot, and S. Brown, Primary production, new production, and growth rate in the equatorial Pacific: Changes from mesotrophic to oligotrophic regime, *J. Geophys. Res., 108*(C12), 8141, doi:10.1029/2000JC000914, in press, 2003.

Lukas, R., and E. Lindstrom, The mixed layer of the western equatorial Pacific Ocean, *J. Geophys. Res., 96*, 3343–3357, 1991.

Marra, J., Analysis of diel variability in chlorophyll fluorescence, *J. Mar. Res., 55*, 767–784, 1997.

Moore, L. R., and S. W. Chisholm, Photophysiology of the marine cyanobacterium *Prochlorococcus*: Ecotypic differences among cultured isolates, *Limnol. Oceanogr., 44*, 628–638, 1999.

Moore, L. R., R. Goericke, and S. W. Chisholm, Comparative physiology of *Synechococcus* and *Prochlorococcus*: Influence of light and temperature on growth pigments, fluorescence and absorptive properties, *Mar. Ecol. Prog. Ser., 116*, 259–275, 1995.

Neveux, J., and F. Lantoine, Spectrofluorometric assay of chlorophylls and phaeopigments using the least squares approximation technique, *Deep Sea Res., Part A, 40*, 1747–1765, 1993.

Owens, T. G., P. G. Falkowski, and T. E. Whitledge, Diel periodicity in cellular chlorophyll content in marine diatoms, *Mar. Biol., 59*, 71–77, 1980.

Partensky, F., N. Hoepffner, W. K. W. Li, O. Ulloa, and D. Vaulot, Photoacclimation of *Prochlorococcus* sp. (Prochlorophyta) strains isolated from the North Atlantic and the Mediterranean Sea, *Plant Physiol., 101*, 295–296, 1993.

Post, A. F., Z. Dubinsky, K. Wyman, and P. G. Falkowski, Kinetics of light-intensity adaptation in a marine planktonic diatom, *Mar. Biol., 83*, 231–238, 1984.

Post, A. F., Z. Dubinsky, K. Wyman, and P. G. Falkowski, Physiological responses of a marine planktonic diatom to transitions in growth irradiance, *Mar. Ecol. Prog. Ser., 25*, 141–149, 1985.

Ricketts, T. R., Magnesium 2,4-divinylphaeoporphyrin a5 monomethyl ester, a protochlorophyll-like pigment present in some unicellular flagellates, *Phytochemistry, 5*, 223–229, 1966.

Roman, M. R., H. G. Dam, A. L. Gauzens, J. Urban-Rich, D. G. Foley, and T. D. Dickey, Zooplankton variability on the equator at 140°W during the JGOFS EqPac study, *Deep Sea Res., Part II, 42*, 673–693, 1995.

Setser, P. J., N. L. Uinasso, and D. R. Shink, Daily patterns of fluorescence in vivo in the central Pacific Ocean, *J. Mar. Res., 40*, 453–471, 1982.

Sherr, B. F., E. B. Sherr, and R. D. Fallon, Use of monodispersed, fluorescently-labeled bacteria to estimate in situ protozoan bacterivory, *Appl. Environ. Microbiol., 53*, 958–965, 1987.

Siegel, D. A., T. D. Dickey, L. Washburn, M. K. Hamilton, and B. G. Mitchell, Optical determination of particulate abundance and production variations in the oligotrophic ocean, *Deep Sea Res., Part A, 36*, 211–222, 1989.

Sournia, A., Circadian periodicities in natural populations of marine phytoplankton, *Adv. Mar. Biol., 12*, 325–389, 1974.

Strom, S. L., C. B. Miller, and B. W. Frost, What sets lower limits to phytoplankton stocks in high-nitrate, low-chlorophyll regions of the open ocean?, *Mar. Ecol. Prog. Ser., 193*, 19–31, 2000.

Suzuki, L., and C. H. Johnson, Algae know the time of the day: Circadian and photoperiodic program, *J. Phycol., 37*, 933–942, 2001.

Vaulot, D., CYTOPC: Processing software for flow cytometric data, *Signal Noise, 2*, 8, 1989.

Vaulot, D., and D. Marie, Diel variability of photosynthetic picoplankton in the equatorial Pacific, *J. Geophys. Res., 104*, 3297–3310, 1999.

Vaulot, D., D. Marie, R. J. Olson, and S. W. Chisholm, Growth of *Prochlorococcus*, a photosynthetic prokaryote, in the equatorial Pacific Ocean, *Science, 268*, 1480–1482, 1995.

Verity, P. G., D. K. Stoecker, M. E. Sieracki, and J. R. Nelson, Microzooplankton grazing of primary production at 140°W in the equatorial Pacific, *Deep Sea Res., Part II, 43*, 1227–1255, 1996.

Vesk, M., and S. W. Jeffrey, Ultrastructure and pigments of two strains of the picoplanktonic alga *Pelagococcus subviridis* (Chrysophyceae), *J. Phycol., 23*, 322–336, 1987.

Walsh, I. D., S. P. Chung, M. J. Richardson, and W. D. Gardner, The diel cycle in the integrated particle load in the equatorial Pacific: A comparison with primary production, *Deep Sea Res., Part II, 42*, 465–477, 1995.

Yentsch, C. S., and R. F. Scagel, Diurnal study of phytoplankton pigments. An in situ study in East Sound, Washington, *J. Mar Res., 17*, 567–583, 1958.

Zapata, M., B. Edvarsen, F. Rodriguez, M. A. Maestro, and J. L. Garrido, Chlorophyll *c*2 monogalactosyldiacylglyceride ester (chl *c*2-MGDG). A novel marker pigment for *Chrysochromulina* species (Haptophyta), *Mar. Ecol. Prog. Ser., 219*, 85–99, 2001.

J. Blanchot, Institut de Recherche pour le Développement (IRD)-Sainte Clotilde, St. Clotilde, 97940 La Réunion, France.

S. L. Brown and M. R. Landry, Department of Oceanography, University of Hawaii at Manoa, 1000 Pope Rd., Honolulu, HI 96822, USA.

C. Dupouy, LODYC (CNRS-IRD-UPMC), UMR 7617, UPMC, 4 Place Jussieu, 75452 Paris, France.

A. Le Bouteiller, IRD-Nouméa, BP A5, Nouméa, 98848 Nouvelle Calédonie.

J. Neveux, Observatoire Océanologique de Banyuls (CNRS-UPMC), Laboratoire Arago (UMR 7621), BP44, 66651 Banyuls sur Mer, France. (jneveux@obs-banyuls.fr)

Neveux J., Dupouy Cécile, Blanchot Jean, Le Bouteiller Aubert, Landry M.R., Brown S.L. (2003)

Diel dynamics of chlorophylls in high-nutrient, low-chlorophyll waters of the equatorial Pacific (180°) : interactions of growth, grazing, physiological responses and mixing

In: A JGOFS investigation of plankton variability and trophic interactions in the central equatorial Pacific (EBENE)

Journal of Geophysical Research, 108 (C12), 5-1 - 5-17

ISSN 0148-0227